

# **Creation of a Digital Geological Map Dataset of Marie Byrd Land, Antarctica**

**A Senior Thesis Presented to the Department of Geology**

Bachelor of Arts

**Samuel Elkind**

Colorado College

May 2016

## Table of Contents

<b>Abstract.....</b>	<b>3</b>
<b>Introduction .....</b>	<b>4</b>
<b>Geological Background .....</b>	<b>6</b>
<b>Methods.....</b>	<b>10</b>
<b>Surface Geology and Geospatial Framework .....</b>	<b>10</b>
<b>Geophysical data and mapping of subglacial contacts .....</b>	<b>12</b>
<b>Results.....</b>	<b>14</b>
<b>Geological dataset.....</b>	<b>14</b>
<b>Geophysical domains .....</b>	<b>15</b>
<b>Discussion.....</b>	<b>17</b>
<b>Swanson Formation .....</b>	<b>17</b>
<b>Pleistocene Volcanics .....</b>	<b>17</b>
<b>Metamorphic Core Complexes .....</b>	<b>19</b>
<b>Regional Kinematics .....</b>	<b>21</b>
<b>Conclusion .....</b>	<b>21</b>
<b>Works Cited.....</b>	<b>22</b>
<b>Figures.....</b>	<b>26</b>

## Abstract

Bedrock exposures are relatively sparse in Marie Byrd Land (MBL), due to the presence of extensive sheet, but provide important constraints on the nature of sub-ice geology of West Antarctica. The most extensive area of outcrops are found in the Ford Ranges and Edward VII Peninsula, bordering the Ross Sea and Ice Shelf. We used ground-based geological observations to develop the first digital geological map for Marie Byrd Land, as a component of the new SCAR GeoMap project (<http://www.scar.org/geomap>). The map covers a coastal area of 250 km<sup>2</sup> between 140°E to 160°E, from 75°S to 80°S, at around 1:250 000 scale. Exposed rock is delimited by 911 polygons, occupying 250 km<sup>2</sup> that comprises 0.2% of the total area. Supraglacial features and glacial till, together with seasonal water and blue ice, also are distinguished within the digital map, due to their relevance to ice sheet history and dynamics. There are 119 mapped till deposit polygons (11.2 km<sup>2</sup>), 58 supraglacial tills (5.7 km<sup>2</sup>) and 69 seasonal water features (21.5 km<sup>2</sup>) that provide a baseline for past and future glaciological change. Rendered in geographic information system software Esri© ArcMap, the GIS will be made publically available as an ArcGIS map service and Google Earth files.

Using the new GIS, an interpretive map of sub-glacial bedrock geology has been generated for the region, drawing upon archival airborne geophysical data (magnetics, gravity, ice thickness, and sub-ice topography) recorded at 5.3 and 10.6 km line spacing over the Ford Ranges (Luyendyk et al., 2003), augmented by marine bathymetry. Polygon features correspond to geological formations, and line features to inferred crustal faults at regional scale. Six fault classifications reflect the strength of the basis for the inference of the subglacial structure, based on criteria including active seismicity, topographic or ice surface lineament, and steep gravity or magnetic gradients. Pliocene and younger volcanism, zones of inferred mineralization/geothermal activity, and glacial deposits were mapped with extreme care due to their potential consequences for ice sheet stability. The current configuration is rendered upon BEDMAP2 subglacial topography and an alternative view is projected onto adjusted topography following glacial rebound (after Wilson et al. 2012). The re-examination of archival data is timely within ongoing geophysical exploration and dataset compilation for Antarctica, such as SCAR ADMAP, NASA Icebridge, and POLEnet. The new subglacial framework and deeper understanding of bedrock structure in MBL is used to test existing hypotheses about the tectonic evolution and identify factors that may affect ice sheet stability. It provides a geological context for the eastern boundary of the Ross Ice Shelf region being mapped by the 2015-2018 USAP ROSETTA-Ice airborne geophysical investigation.

## **Introduction**

Marie Byrd Land, Antarctica (Figure 1), is a glaciated region affected by atmosphere and ocean warming, with the potential to contribute to sea-level rise (e.g. Rignot et al. 2014). If deglaciation scenarios play out rapidly, it will be valuable to have consolidated information about the subglacial bedrock geology of the region, including factors that may influence the manner and location of glaciological change. Marie Byrd Land has a legacy of tectonic extension as part of the West Antarctic Rift System (WARS). As a result, this region has significantly thinner crust than the rest of the continent (Figure 2). Interpretation of airborne geophysics is one avenue to discover tectonically derived structures that are responsible for the crustal attenuation. Evidence from geophysical potential fields data and geological mapping indicate factors, including subglacial volcanism (quiescent; Luyendyk et al. 2003), fault zones (Stypula, 2009), zones of mineralization attributable to geothermal activity (Siddoway, unpublished), and high heat-flow (e.g. Fisher et al., 2015), that, in concert with ongoing warming of ocean and atmosphere in polar regions, may have bearing on future changes in volume and dynamics of the West Antarctic Ice Sheet (WAIS I present the first subglacial bedrock map of West Antarctica interpreted from geological and geophysical data collected between 1998-2012 (Figure 3) and augmented by findings from current POLEnet seismology investigations ([polenet.org](http://polenet.org)).

An additional cause of concern is active seismicity. In 2012, four earthquakes between magnitude 4.4 and 5.5 occurred north of Edward VII Peninsula (Figure 4) (e.g. event 201206010507A, [www.globalcmt.org](http://www.globalcmt.org)), a landmass that borders the eastern margin of the Ross Ice Shelf. These events were the first moderate magnitude earthquakes ever recorded in the continental crust (as distinguished from oceanic lithosphere) of Antarctica

([http://earthquake.usgs.gov/earthquakes/eventpage/usp000jm6p#general\\_summary](http://earthquake.usgs.gov/earthquakes/eventpage/usp000jm6p#general_summary)). Seismic activity of this magnitude, elsewhere, can be a trigger for migration of magma or geothermal fluids, and/or for perturbations in heat flow and strain (Walter et al., 2009). Elsewhere, in the Executive Committee Range, a study by Lough et al. (2013) interpreted swarms of minor seismic activity as evidence for activity within a sub-glacial magmatic complex, as a potential precursor to a volcanic eruption. These two classes of geological activity stem from the region's extensional tectonic history (Siddoway, 2008) and current plate dynamics (Paulsen and Wilson, 2010).

As anthropogenic climate change progresses (Rignot et al. 2014), the need for a profound understanding of the complex dynamics of the WAIS, including the subglacial geotectonic elements, is becoming critical. My senior thesis integrates information from geological maps of western Marie Byrd Land (MBL) and potential fields data (airborne magnetics, gravity, ice thickness, and sub-ice topography) to 1) contribute to the first geological map webservice for a large region of Antarctica, as a collaboration with Simon Cox at GNS Science, New Zealand, and Polar Geospatial Center, Univ. Minnesota, and 2) create the first bedrock geological map of Antarctica rendered upon a) BEDMAP2 subglacial topography (<https://www.bas.ac.uk/project/bedmap-2/#about>) and b) adjusted topography following glacial rebound (Wilson et al., 2012). The maps, at 1:250 000 scale in the geographic information system (GIS) software ArcMap, depict formation contacts, fault contacts, sites and extent of Pliocene and younger volcanism, and zones of mineralization/geothermal activity. The point of departure for the sub-glacial bedrock map of western Marie Byrd Land is the existing comprehensive database of geological and geophysical data assembled by C. Siddoway and students between 2005-2012 (e.g. Stypula, 2009; Cowling, 2010; Emery, 2011;

[The questions I seek to address in the course of this undertaking include: What do spatial relationships between faults, intrusive bodies, and core complexes reveal about the kinematics of the region? Can all geophysical signatures in the available dataset be categorized into the known geological units or if an unknown unit must be included?](http://sites.coloradocollege.edu/csiddoway/antarctica-research/)

This new interpretation contributes to newly funded ROSETTA-ICE research, that aims to map the bedrock and bathymetry beneath the Ross Ice Shelf (<http://www.sciencemag.org/content/348/6239/1070.full?sid=236f399f-90d3-45bf-acfb-d5fdf098cf5f>), and to the GEOMAP project of the Scientific Committee on Antarctic Research (<http://www.scar.org/geomap>) that will expand the scientific understanding of the continent beyond the current limited extent of the outcrops in sparse nunataks to the broad sub-glacial bedrock domains.

A detailed map of the study region in West Antarctica that covers both exposed and sub-ice bedrock is of value for glaciologists and climate scientists who strive to identify vulnerable sectors of the WAIS in order to forecast the effects of climate warming, and for geologists who wish to test hypotheses about the tectonic events that shaped the geology of West Antarctica. These events include the opening of the West Antarctic Rift System and the breakup between New Zealand and West Antarctica that led to opening of the Southern Ocean (Storey et al., 1998; Siddoway, 2008). This undertaking provides a resource to improve our understanding of the region's tectonic past, and may contribute to modeling of the region's glacial future.

## **Geological Background**

A region of extensive rock outcrops is the Ross Province, in western Marie Byrd Land (Figures 5, 6). The task of mapping subglacial bedrock is made feasible by the limited geological variety

and by comparison with geologically correlative regions that exist in North Victoria Land, eastern Australia, and New Zealand. The known formations are early Paleozoic low-grade greywacke and argillite of the Swanson Formation, Devonian Ford Grandiorite, Cretaceous Byrd Coast Granite, Cretaceous mafic dikes, and minor Neogene volcanic rocks, primarily basalt (Luyendyk et al., 2003; Siddoway, 2008). In addition there are two known complexes of migmatite gneiss, one extensive and derived from the first four of those units, together (Siddoway et al. 2004; Yakymchuk, 2015), and the other, of limited extent, that is a derivative of late Paleozoic sedimentary rocks of which little is known (Pankhurst et al. 1998).

The Swanson Formation is a widespread, thick succession of turbidite deposits from the Cambrian-Ordovician Periods (Bradshaw et al., 1983; Adams, 2004). This unit has been subjected to subgreenschist-greenschist metamorphism and exhibits large scale folding (Figure 7). Marie Byrd Land was once contiguous with North Victoria Land, the continental plate of Zealandia, and eastern Australia, and Swanson-equivalent formations exist in each of these regions. These are the Robertson Bay Group, the Greenland Group and, the Lachlan Group, respectively (Ireland et al., 1998; Pankhurst et al., 1998; Adams, 2004; Yakymchuk et al., 2015). Large-scale variations in quartz versus clay (now, chlorite) content, and amount of carbonate, are a consequence of the processes of turbidite deposition.

Based upon mica cleavage ages in the Swanson Formation, the wide scale folding (Figure) occurred from contraction between 448 and 444 Ma (Adams, 2004). Following this the Ford Granodiorite intruded the Swanson Formation in the beginning of the Devonian and continuing into the Carboniferous (Yakymchuk et al. 2015). The Ford Granodiorite is a suite of metaluminous to weakly peraluminous, calc-alkaline, I-type granodiorite to monzogranite rocks. The melt forming the Ford Granodiorite was generated by subduction along the active

convergent continental margin of Gondwana (Weaver et al., 1991). This suite of rocks was emplaced in at least two phases, with I-type granodiorites at 375-350 Ma age and lesser S-type products of crustal anatexis between 350-338 Ma (Pankhurst et al., 1998; Yakymchuk et al. 2015). The first phase correlates with the Admiralty Intrusives of North Victoria Land, Antarctica (Muir et al., 1996) as well as the Karamea Batholith in New Zealand (Tulloch et al., 2009). The second phase has similar characteristics to S-type granitoids intruding into Lachlan metasediments in Australia (Figure 8; Hallett et al., 2005).

The Byrd Coast Granite is Cretaceous-age alkali to calc-alkaline granite that intrudes the Swanson Formation, Ford Granodiorite, and Fosdick Mountains migmatite. These A-type granitoids represent the main plutonic phase emplaced during activation of the West Antarctic Rift System; a significant change from the previous convergent tectonic setting (Weaver et al., 1994; Brown et al., in review). Mafic dikes also intruded the region in Cretaceous time, overlapping in time with earlier-intruded Byrd Coast intrusions (Saito et al. 2011). Unroofing during regional extension exposed deep-level metamorphic core complexes (MCCs) in the Fosdick Mountains and the Alexandra Mountains (Siddoway et al., 2004; McFadden et al., 2010).

One such MCC, the Fosdick migmatite complex consists of midcrustal rocks that enjoyed high temperature conditions during prograde metamorphism which caused partial melting in preexisting rock. The temperature and pressure conditions reached amphibolite to granulite facies, affecting Swanson Formation and Ford Granodiorite. Diverse leucogranites and Byrd Coast Granite are the products of anatexis (Brown et al., in review). Visible today in the Fosdicks are paragneisses, orthogneisses, sheeted leucogranites and undifferentiated migmatite derived from combinations of these rock units (Siddoway, 2008). The most recent period of

metamorphism peaked around from 106 to 99 Ma, which coincides with intracontinental extension across the continental margin of Gondwana; this was succeeded by rifting and breakup between Zealandia and Antarctica (Siddoway et al., 2004).

Competing hypotheses from Siddoway (2008) and Storey et al. (1999) seek to explain the mechanisms that drove the greater than 100% extension in the West Antarctic Rift System prior to the breakup between West Antarctica and Zealandia. Storey et al. (1999) proposes that the continental spreading and magmatism was catalyzed by heat from a mantle plume that still persists, and now underlies the Ross Sea. Alternatively, Siddoway (2008) suggested that an elevated thermal gradient developed due to aesthenospheric circulation in the mantle wedge subduction zone of the convergent margin, leading to partial melting and lateral flow in the middle and lower crust, a situation that has been modeled by Rey and Müller (2010). . The overriding plate in MBL underwent oblique transtension, with kinematics linked to oblique subduction of the Phoenix oceanic plate (Sutherland and Hollister, 2002).

Storey et al. (1999) and LeMasurier and Landis (1996) also suggests the presence of a mantle plume directly below Marie Byrd Land to account for the Cenozoic alkaline basalts. These Pleistocene volcanic outcrops occur in dikes, cinder cones and lava flows (Gaffney and Siddoway, 2007). While there is limited sub-aerial exposure of these rocks, an extensive volcanic field to the East of the Fosdick Mountains has been proposed by Luyendyk et al. (2003) based upon high frequency, high amplitude geophysical anomalies.

Accordance with USGS and international mapping protocols, basic geological maps for West Antarctica portray geological information and bedrock identity only where there are rock exposures emergent from the extensive ice cover of the West Antarctica ice sheet (WAIS). In western Marie Byrd Land (MBL) there is fairly abundant rock exposed in the Ford Ranges that

provides “ground truth” for a bedrock geology map to be constructed in GIS. Airborne geophysical surveys were done over the Ford Ranges, so total magnetic field intensity, free air gravity, Bouger gravity, and ice penetrating radar data exist for the area. Each of the rock units has a different geophysical and spectral “signature,” due to differences in density and magnetic mineral content (Luyendyk et al., 2003), which can be used to map out the sub-ice extent of rock formations, formation contacts, fault zones and possibly folds. A small number of faults that formed during development of the West Antarctic Rift system (WARS) are known from geology field studies (Siddoway, 2008), but this project reveals many more that are expressed as ‘lineaments’ in the gravity, magnetics, and/or radar data. Of immediate interest are the faults that accommodated M4 to M5 seismicity in 2012 (see above) and associated structures.

Airborne geophysics and airborne magnetics were collected for a 470 km by 530 km area over the Ford Ranges in western MBL (Luyendyk, et. al 2003). Flight lines had 15 km spacing in most of the study area with 10 km spacing over smaller sections. Gravity modeling indicates regions of low-density rock in the subsurface that contrast with metamorphic and plutonic rock of intermediate density exposed at the surface of MBL; the low density material may be glacial deposits or weakly lithified Cenozoic or older sedimentary deposits. Aeromagnetics reveal high amplitude anomalies that likely correspond to sub-ice volcanic provinces (Luyendyk, et. al 2003), that may be sites of elevated heat flow or renewed eruption that is of consequence for ice sheet stability.

## Methods

### Surface Geology and Geospatial Framework

The identity of bedrock outcrops in western Marie Byrd Land have been determined from a multitude of sources (e.g. Wade et al., 1977; Pankhurst et al., 1998; Ferraccioli et al., 2002;

Siddoway et al., field mapping). The polygon vector coverage of the outcrops was digitized by hand using the perimeter of outcrops visible in panchromatic Digital Globe imagery from QuickBird, WorldView 1 and, WorldView 2 satellites. Because these photos were taken at different times and from different positions, orthorectification of the images does not result in perfect positional accuracy or consistency for features depicted from one image to another. Positional errors were, on average, in the tens of meters, but occasionally were as high as 200m. To compensate, the positions of the outcrops were adjusted to align with the Landsat Image Mosaic of Antarctica (LIMA; available through the USGS (<http://LIMA.usgs.gov>)). The LIMA Thematic Mapper images are accurately georegistered and display the most accurate, publicly available representation of snow cover and exposed bedrock in the region within a universal spatial reference frame. While no projected dataset is 100% accurate, this approach preserves the high quality geometrical detail attainable from high-resolution satellite imagery with the congruence of a spatial frame that LIMA provides. In some cases, outcrop margins were generalized to better represent map relationships or to improve visibility of key geological units at the 1:250,000 scale.

Glacial till was introduced as a geological formation with three subdivisions reflecting the geological context. Till exposures were located and digitized upon fairly high resolution Digital Globe imagery available in Google Earth (Figure 9), together with panchromatic high-resolution imagery. The observable characteristics of neighboring bodies of ice, and relative age relationships with other tills were the main factors considered when determining the attribution of these features.

The polygon coverage, along with line features representing faults, line representing features dikes, and point features representing structural data, were formatted and classified to

conform to GeoSciML standards. GeosciML or Geoscience Markup Language is a formal schema for organizing geological data. Developed and managed by the Commission for the Management and Application of Geoscience Information (CGI), it is designed to facilitate interoperability and sharing of datasets. To adopt GeoSciML formatting, the attributes tables of our vector data were edited. In this process, some relevant information was lost (ie: site specific descriptive information) due to the strictly regulated schema, but the compatibility gained in this process dramatically increases the possibility of collaborative efforts to further analyze this data; the objective of global scale digital datasets. The adherence to international GeoSciML protocols will allow for easy queries of data according to attributes in the database. The data were projected in ArcMap 10.3.1 in the WGS 1984 Antarctic Polar Stereographic projected coordinate system. This coordinate system is used for all data in this study.

A topology of the geological polygons was constructed to ensure that all gaps between polygons were intentional, and that there were no overlaps between geological units. This is an essential part of the process for both aesthetic reasons and for the potential use of these polygons for zonal statistics.

### Geophysical data and mapping of subglacial contacts

The airborne geophysical data from Luyendyk et al. (2003) were downloaded from [http://www-udc.ig.utexas.edu/external/facilities/aero/data/soar/WMB/SOAR\\_wmb.htm](http://www-udc.ig.utexas.edu/external/facilities/aero/data/soar/WMB/SOAR_wmb.htm) and brought into ArcMap as three dimensional point features (latitude, longitude, and data value). These data include bed elevation for subglacial topography, ice surface elevation from radar, free air gravity, magnetic field intensity, and Bouger gravity. The point features were converted to raster layers using ArcMap's Point to Raster conversion tool. A mean cell assignment and cell

size of 2700m were the parameters for the tool. To display the data for interpretation, bilinear interpolation was used as a resampling method. I found that the “Aspect” color ramp provided the best visual portrayal of the potential field data.

Anomalies in Earth’s magnetic field are caused by a combination of the magnetic susceptibility of rocks in the crust and of the remnant magnetism in the rock. Both of these factors are mainly influenced by the amount of ferromagnetic material contained in the rock. Magnetic susceptibility will vary within a rock unit due to compositional differences, but if the range of values is known for a rock unit it can be used to construct part of a geophysical signature for that rock type. Fairly comprehensive magnetic susceptibility data for western MBL are reported by Ferraccioli et al. (2002; Figure 10).

Variation in gravitational field data is caused by the distance from the center of the Earth, and changes in the amount of material and density of that material between the gravimeter and the center of the earth. Free air gravity is corrected for the elevation distance above (or below) sea level. Gravity anomalies from free air gravity are due to changes in topography and composition of the crust. Bouger gravity is data that has been corrected by accounting for the amount of mass in the terrain that is above/below sea level. This mass is estimated by assuming an average rock density for the region, and multiplying that by the volume of material above sea level based upon bed elevation data. In this case, ice thickness data were used in conjunction with an average density that has been adjusted to account for the ice sheet. The remaining variations in the gravitational field are due to variations in density in the bedrock of the region. The interpreted density of the regional geologic units is another valuable characteristic in the geophysical signature of the rock types that factors into the interpretation of subglacial geology.

As an aid to identifying trends in the magnetic anomaly data, a magnetic gradient layer was generated in ArcMap using the Slope Data Analysis tool. Magnetic gradient is the final component in creating a complete geophysical signature. Lineaments marking the position of steep magnetic gradients potentially are associated with geological faults that juxtapose units with contrasting physical characteristics (e.g. Finn and Sims, 2005). Using these geophysical signatures of the rock types as well as “ground truth” outcrop geology, interpolation of subglacial bedrock types and locations of structures is possible through classification of the geophysical domains.

There is great potential to test existing hypotheses (Luyendyk et al. 2003; Siddoway, 2008) and obtain a deeper understanding of the bedrock structure of MBL by examining the SOAR wMBL survey data within the new context that has emerged from ongoing geophysical exploration in Antarctica over the past 15 years. As a final step in the geophysical analysis, the 25,000 km<sup>2</sup> area of wMBL is examined within the context of the ADMAP magnetic data compilation of Antarctica (<http://www.martagh.com.ar/ADMAP/>), NASA Icebridge datasets for WANT ([https://www.nasa.gov/mission\\_pages/icebridge/index.html](https://www.nasa.gov/mission_pages/icebridge/index.html)), and the preliminary magnetics and gravity data obtained by ROSETTA-Ice (unpublished), in order to identify pronounced regional trends that are attributable to the extent of bedrock formations and faults.

## Results

### Geological dataset

The dataset compiled from field data and analysis of high resolution satellite imagery includes polygon coverage of rock outcrops, line coverage of inferred faults and point coverage of structural measurements. The map covers an area of 135,000 km<sup>2</sup>. 911 polygons delimit the

250 km<sup>2</sup> of exposed rock (0.2% of the total area). 119 of those are till deposits, 58 are supraglacial tills, and 69 are seasonal bodies of water. 80 inferred faults have been included in the dataset. Classification of a fault required some combination of active seismicity, topographic lineament, and steep gravity or magnetic gradients. The faults have been divided into six classes based upon the strength of the interpretation. The 1,086 structural points include measurements of bedding, cleavage, axial planes, foliation, lineations, folds, shears and, veins (Figure 11).

### Geophysical domains

Large sections of the aeromagnetic map are magnetically “quiet” (Figure 12). They represent a magnetic “baseline” from which other anomalies become apparent.

One class of geophysical features that is distinct from the magnetic baseline consists of very high magnitude (>350nT), very short wavelength (<15km) magnetic anomalies (Figure 12, 13). These features are sub-circular in shape and have very high magnetic gradients. The Bouger gravity and topography show limited to no spatial correlation to these magnetic features. 18 features matching these characteristics have been identified in the mapping area (Figure 14). The average size of these features is 262.34 km<sup>2</sup>. The largest and smallest features have areas of 2578.6 km<sup>2</sup> and 14.75 km<sup>2</sup> respectively. In total, the anomalies make up 3.43% of the total map area. Ten of these features are located in a loose grouping in the north east quadrant of the area. One larger anomaly with several local highs is located in the south central portion of the map.

A second set of geophysical features include both short and long wavelength, low gradient, low to moderate magnitude (100-300 nT) magnetic anomalies (Figures 15,16,17). The Bouger signature does not exhibit any discrete spatially associated anomalies. Topographic

correlation is apparent for some, but not all of the regions. This set consists of 20 features with widely variable sizes (Figure 18). The average size is 1531.87 km<sup>2</sup>. The largest and smallest features have areas of 6130.98 km<sup>2</sup> and 42.40 km<sup>2</sup> and they account for 18.94% of the total area. Perplexingly, the majority of the features are located on the northern half of the map area and clustered in the north east corner.

A final distinct group of geophysical features can be classified as moderate magnitude (200-300 nT), moderate wavelength (20-30km) magnetic anomalies (Figure 19). They are elongate or sub-circular and have moderate magnetic gradients (much lower than the high-magnitude anomalies). In some cases, the magnetic gradient perpendicular to the long axis of the feature is more gradual on one side than the opposite side. Interestingly, one set of four anomalies form a linear chain oriented roughly 30 degrees west of north (striking 330-150). A second, larger and single elongate anomaly that underlies outcrops of high grade metamorphic rocks making up the Fosdick migmatite dome has an orientation striking 98-278 E-W. Topography shows strong correlation to these magnetic features. In all but one case a topographic high is slightly offset from the magnetic high. It is difficult to determine with certainty if Bouger gravity values exhibit an associated positive anomaly due to gaps in the data for most of the features, but some of the features that do have sufficient data appear to have Bouger highs loosely related to the magnetic highs with magnitudes between 5mGals and 20 mGals. In total, 8 anomalies display these geophysical characteristics (Figure 20). The average size of these features is 892.83 km<sup>2</sup>. The largest and smallest features have areas of 2546.82 km<sup>2</sup> and 131.10 km<sup>2</sup> and they account for 5.20% of the map area. Included in this set are two magnetic highs on Edward VII Peninsula interpreted by Ferracioli et al. (2002) as bodies of Ford Granodiorite. However, the magnitude of the magnetic anomalies along with outcropping

metamorphic rock points towards an alternative interpretation consistent with this second class of features.

## **Discussion**

### Swanson Formation

The baseline magnetically quiet regions are interpreted to be the metasedimentary Swanson Formation. This unit should have the most homogenous composition with limited ferromagnetic material relative to the other units. I concur with Luyendyk et al.'s (2003) assessment that long wavelength variations in magnetic intensity are likely due to compositional heterogeneity of the unit. Thanks to the similar densities of the most prevalent units: the Byrd Coast Granite, the Ford Granodiorite, and the Swanson Formation, it is likely that the map-scale variations in the Bouger gravity are controlled by crustal thickness rather than variations in the bedrock.

### Pleistocene Volcanics

My interpretation of the short wavelength, high magnitude, and high gradient magnetic anomalies is consistent with the interpretations of Luyendyk et al., (2003) and Stypula (2009). This set of magnetic anomalies without any related gravity or topography anomalies can most easily be explained by a small, very near surface body with a very high magnetic susceptibility. These are likely geophysical expressions of volcanic plugs likely of Cenozoic age who's highly mafic material accounts for the magnetic anomaly, but erosion of the volcanoes themselves prevents the very dense material from affecting the Bouger gravity. An additional factor which could obscure the gravitational signature of the anomalies in the eastern quadrant of the map is the isostatic compensation of high topography. The gravitational signature of the generally

thicker crust in this region (~31 km) (Luyendyk et al, 2003) could obscure any gravity anomaly caused by the near surface mafic material.

One outlier in this group of anomalies is described by Ferraccioli et al., (2002) as high-amplitude, linear and short-wavelength feature located in Sulzberger Bay (Figure 21). The anomaly differs from the other in shape. Instead of sub-circular, it is elongate. This is typical of shallow-source magnetic anomalies located over Cenozoic rocks of the McMurdo Volcanic Group in North Victoria Land (LeMasurier and Thompson, 1990). The linear trend along which this is emplaced is commonly interpreted as WANT rift fabric (Behrendt et al., 1996). The orientation of this feature trends roughly 129-309 NW-SE, suggesting a direction of extension of 39-219 NE-SW. Additional support for this interpretation is the proximity of this feature to a regional-scale inferred fault that recently experienced 4 earthquakes in 2012. Analysis of one of these earthquakes on 6/1/2012, 5:7:5.8 GMT which had a magnitude of 5.5 yielded a south dipping fault plane, striking 107. The distinction between nodal plane and fault plane was decided on the basis of regional crustal structure and the distribution of M4 and 5 faults by C. Siddoway. The earthquake was a normal faulting earthquake with a component of left-lateral strike slip motion (Doug Wiens and A. Nyblade, Personal communication). The magnetic anomaly is located north of the epicenter of this particular earthquake and is subparallel to the inferred northern segment of the fault.

#### Intrusive bodies (Byrd Coast Granite, Ford Granodiorite)

The third group of geophysical features consists of low gradient, low magnitude magnetic anomalies with no associated Bouger trends. Generation of these anomalies requires material that is of similar density to the surrounding geology but has a slightly higher magnetic susceptibility.

Both the I-type granitoids of the Ford Granodiorite Suite and the A-type granites of the Byrd Coast Granite fit these parameters. On the basis of geophysics alone, these two units are indistinguishable and have been classified together as “intrusive plutonic bodies”. In some cases, especially in the Ford Ranges, groundtruth allows for separation of these features into either Ford or Byrd Coast, but for sub-ice region, this distinction is impossible.

### Metamorphic Core Complexes

The class of geophysical features with moderate magnitude, medium wavelength magnetic anomalies and correlated Bouger and topographic highs require that the bedrock affecting these potential fields is higher in both density and magnetic susceptibility than the surrounding geology. These conditions are satisfied by the properties of the outcropping rock in the Fosdick Mountains, which is located directly on top of one such anomaly. The sheeted leucogranites, Swanson paragneiss, Ford orthogneiss and other undifferentiated migmatites found in this mountain range are both denser, and richer in mafic material than the surrounding Byrd Coast Granite, Ford Orthogneiss, and Swanson Formation. These highly metamorphosed rocks make up the EW trending Fosdick Migmatite Dome (FMD). The FMD is bounded on the south by a south dipping, dextral-oblique detachment zone (Mcfadden et al. 2007) and on the north by an inferred steep dextral strike slip zone (Siddoway et al., 2004b). This arrangement of faults around an exhumed metamorphic core complex is similar to the Catalina core complex (Terrien, 2010; Carol Finn, Personal communication) and fits with the general model for core complexes as established by Platt et al. (2014) (Figure 22). Metamorphic Core Complexes are the result of extreme crustal extension and attenuation achieved by low angle normal faulting. Faulting initializes at about 30 degrees but rotation associated with the faulting reorients the fault

plane to a much lower angle until it becomes inactive. Following this, a new fault initializes at 30 degrees and the process continues until it results in unroofing of mafic material from the mid to lower crust, from below the brittle-ductile boundary. The removal of the lithostatic load from the exhumed material results in isostatic doming. The orientation of metamorphic core complexes is almost always orthogonal to the direction of extension. However, in the case of the FMD, the dextral oblique slip of both bounding faults has rotated the feature from its original position.

Elsewhere, in the south-central region of the map, a chain of four features which conform superbly to the geophysical characteristics expressed above (Figure 19) are aligned in a trend of 330- 150 NW-SE. This would supply a direction of extension of 60-240 NE-SW. This is very similar to the orientations of a host of mafic dikes that are of 104-96 Ma age and trend close to 344 (Siddoway et al., 2005). Additionally, the trend of this proposed MCC is sub parallel to the trend of the inferred late Cenozoic volcanic feature described in the previous section. This chain of features is a strong candidate for a metamorphic core complex based upon the geophysical signature and their orientations relative to established kinematic orientations. Additional evidence comes from the sub-ice topography. A profile that crosses this proposed MCC exhibits a moderately dipping slope on the west opposite a gradually dipping slope on the east to form an asymmetrical topographic peak. The moderate slope seems to fit with the breakaway section from established models. The gradual slope resembles the detachment surface. Curiously, in the region above where the hypothesized detachment intersects with the surface, the hanging wall, there is a unique topographic texture. This texture is jagged and irregular. On the basis of available data, only speculation is possible. One possible explanation comes from the Whipple detachment in SE California, who's hanging wall exhibits strikingly similar topography. This

topography is created by truncated volcanic flows and tephras that have been rotated on the listric detachment surface (Figure 23).

## Regional Kinematics

The geological features whose genesis is tectonically controlled include metamorphic core complexes, linear traces of volcanics, and faults (figure 24). The features described above, interpreted based upon geophysical data, all conform to an extensional orientation of ~65 NE as established by regionally distributed mafic dikes. These dikes were all emplaced between 104 and 96 Ma. It is likely that the metamorphic core complex was exhumed during this period of extension. It is also likely that the faults were either initiated, or active during this period and likely accommodated significant strain. However, there is no evidence that the linear trace of sub-ice volcanic rock in Sulzberger Bay was emplaced at this time. More likely, the melt exploited weakness in the crust that were formed during the period of extension and were thus emplaced with similar orientation. However, the recent earthquakes yield a different orientation of extension from these features. The almost due N-S extension of this earthquake is consistent with structures involved in the third phase of extension involving seafloor spreading that separated the Campbell Plateau from wMBL beginning at about 79 Ma (Luyendyk et al., 2003).

## Conclusion

My interpretations of the high-amplitude magnetic anomalies as the result of late Cenozoic volcanism are consistent with the conclusions of Ferracioli et al. (2002) Luyendyk et

al. (2003) and Stypula (2009). I offer a refined interpretation of the locations of Ford Granodiorite and Byrd Coast Granite intrusive bodies from Stypula's (2009) subglacial map. Additionally, I argue for the classification of a linear chain of magnetic anomalies, similar in character of the Fosdick migmatite complex and the Whipple detachment fault, as a metamorphic core complex. Overall, the features I have identified have orientations that fit into the established kinematic regimes of the region and their geophysical signatures can be explained by physical characteristics of known rock units. However, the possibility of new rock units with similar characteristics remains.

Both the digital dataset of surface and subsurface geology open up avenues of future investigation of the Ross Province. These include:

- An independent identification of subglacial faults, using high resolution digital elevation models of the ice surface to identify extensive linear trends in ice fractures that may have geological controls.
- Geophysical investigation of the proposed MCC with higher resolution airborne geophysics
- Spectral analysis of high resolution hyper-spectral (8-band) imagery to identify compositional variations in Swanson Formation metasediments.
- Spectral analysis of high resolution hyper-spectral (8-band) imagery to identify structures (folds) in exposures of high-grade Swanson Paragneiss.

## Works Cited

Adams, C. J. (2004): Rb-Sr age and strontium isotopic characteristics of the Greenland Group, Buller terrane, New Zealand, and correlations at the East Gondwana margin.- New Zealand Journal of Geology & Geophysics, **47**: 189- 200.

An, M., Wiens, D. A., Zhao, Y., Feng, M., Nyblade, A. A., Kanao, M., & Lévêque, J. J. (2015): S-velocity model and inferred Moho topography beneath the Antarctic Plate from Rayleigh waves. *Journal of Geophysical Research: Solid Earth*, 120(1), 359-383.

Behrendt, J. C., Saltus, R., Damaske, D., McCafferty, A., Finn, C. A., Blankenship, D., & Bell, R. E. (1996): Patterns of late Cenozoic volcanic and tectonic activity in the West Antarctic rift system revealed by aeromagnetic surveys. *Tectonics*, 15(3), 660-676.

Brown, C., Yakymchuk, C., Brown, M., Fanning, C.M. Korhonen, F.J., and Siddoway, C.S. (2015): From source to sink: Petrogenesis of Cretaceous anatetic granites from the Fosdick migmatite–granite complex, West Antarctica.- *Journal of Petrology*, **in review**.

Ferraccioli, F., E. Bozzo, and D. Damaske. (2002): Aeromagnetic signatures over western Marie Byrd Land provide insight into magmatic arc basement, mafic magmatism and structure of the eastern Ross Sea rift flank. *Tectonophysics* 347:139-165

Ferraccioli, F., Armadillo, E., Zunino, A., Bozzo, E., Rocchi, S., & Armienti, P. (2009): Magmatic and tectonic patterns over the Northern Victoria Land sector of the Transantarctic Mountains from new aeromagnetic imaging. *Tectonophysics*, 478(1), 43-61.

Finn, C. A., & Sims, P. K. (2005). Signs from the Precambrian: the geologic framework of Rocky Mountain region derived from aeromagnetic data. *The Rocky Mountain Region: An Evolving Lithosphere Tectonics, Geochemistry, and Geophysics*, 39-54.

Gaffney, A. M. and Siddoway, C. S. (2007): Heterogeneous sources for Pleistocene lavas of Marie Byrd Land, Antarctica.- new data from the SW Pacific diffuse alkaline magmatic province (extended abstract).- In Cooper, A. and Raymond, C., eds., *Antarctica.- A Keystone in a Changing World (Proceedings and Conference Abstracts)*: U.S. Geological Survey and The National Academies, USGS OFR-2007-1047, <http://pubs.usgs.gov/of/2007/1047/ea/of2007-1047ea063.pdf>.

Hallett, M., Vassallo, T., Glen, R., Webster, S. (2005): Murray-Riverina region: an interpretation of bedrock Paleozoic geology based on geophysical data. *Geological Survey of New South Wales*,

Ireland, T. R., Flöttmann, T., Fanning, C. M., Gibson, G. M., & Preiss, W. V. (1998): Development of the early Paleozoic Pacific margin of Gondwana from detrital-zircon ages across the Delamerian orogen. *Geology*, 26(3), 243-246.

LeMasurier, W. E., & Thomson, J. W. (1990): Volcanoes of the Antarctic plate and southern oceans (Vol. 48). American Geophysical Union.

LeMasurier, W. E., and C. A. Landis. (1996): Mantle-plume activity recorded by low relief erosion surfaces in West Antarctica and New Zealand. *Bulletin of the Geological Society of America* 108:1450-1466.

Lough, A. C., Wiens, D. A., Barchek, C. G., Anandakrishnan, S., Aster, R. C., Blankenship, D. D., ... & Wilson, T. J. (2013): Seismic detection of an active subglacial magmatic complex in Marie Byrd Land, Antarctica. *Nature Geoscience*, 6(12), 1031-1035.

Luyendyk, B. P., Wilson, D. S., & Siddoway, C. S. (2003): Eastern margin of the Ross Sea Rift in western Marie Byrd Land, Antarctica: Crustal structure and tectonic development. *Geochemistry, Geophysics, Geosystems*, 4(10).

McFadden, R. R., Teyssier, C., Siddoway, C. S., Whitney, D. L., & Fanning, C. M. (2010): Oblique dilation, melt transfer, and gneiss dome emplacement. *Geology*, 38(4), 375-378.

Muir, R. J., Ireland, T. R., Weaver, S. D., & Bradshaw, J. D. (1996): Ion microprobe dating of Paleozoic granitoids: Devonian magmatism in New Zealand and correlations with Australia and Antarctica. *Chemical Geology*, 127(1), 191-210.

Pankhurst, R. J., Weaver, S. D., Bradshaw, J. D., Storey, B. C. and Ireland, T. R. (1998): Geochronology and geochemistry of pre-Jurassic superterrane in Marie Byrd Land, Antarctica. *Journal of Geophysical Research*, 103 (B7): 2529-2547.

Paulsen, T. S., & Wilson, T. J. (2010): New criteria for systematic mapping and reliability assessment of monogenetic volcanic vent alignments and elongate volcanic vents for crustal stress analyses. *Tectonophysics*, 482(1), 16-28.

Rignot, E., Mouginot, J., Morlighem, M., Seroussi, H., & Scheuchl, B. (2014): Widespread, rapid grounding line retreat of Pine Island, Thwaites, Smith, and Kohler glaciers, West Antarctica, from 1992 to 2011. *Geophysical Research Letters*, 41(10), 3502-3509.

Siddoway, C. S., Baldwin, S., Fitzgerald, G., Fanning, C. M. and Luyendyk, B. (2004a): Ross Sea mylonites and the timing of intracontinental extension within the West Antarctic rift system. *Geology*, 32: 57-60.

Siddoway, C. S., Richard, S. M., Fanning, C. M., & Luyendyk, B. P. (2004b): Origin and emplacement of a middle Cretaceous gneiss dome, Fosdick Mountains, West Antarctica. *Geological Society of America Special Papers*, 380, 267-294.

Siddoway, C. S., Sass, L. C. I. and Esser, R. (2005): Kinematic history of Marie Byrd Land terrane, West Antarctica. Direct evidence from Cretaceous mafic dykes. In Vaughan, A., Leat, P. and Pankhurst, J. D., eds., *Terrane Processes at the Margin of Gondwana*, Geological Society of London, Special Publication 246: 417-438.

Siddoway, C. S. (2008): Tectonics of the West Antarctic Rift System: new light on the history and dynamics of distributed intracontinental extension. Antarctica: A Keystone in a Changing World, 91-114.

Siddoway C. and Fanning C.M. (2009): Paleozoic tectonism on the East Gondwana margin.- Evidence from SHRIMP U-Pb zircon geochronology of a migmatite-granite complex in West Antarctica, *Tectonophysics*, **477** (3-4): 262-277, doi:10.1016/j.tecto.2009.04.021.

Storey, B. C., Leat, P. T., Weaver, S. D., Pankhurst, R. J., Bradshaw, J. D., & Kelley, S. (1999): Mantle plumes and Antarctica-New Zealand rifting: evidence from mid-Cretaceous mafic dykes. *Journal of the Geological Society*, *156*(4), 659-671.

Tulloch, A. J., Ramezani, J., Kimbrough, D. L., Faure, K., & Allibone, A. H. (2009): U-Pb geochronology of mid-Paleozoic plutonism in western New Zealand: Implications for S-type granite generation and growth of the east Gondwana margin. *Geological Society of America Bulletin*, B26272-1.

Twiss, R. J. and Moores, E. M. (2007): Structural Geology, 2nd ed. New York: W. H. Freeman and Company, 736 pp.

Walter, T. R., Wang, R., Acocella, V., Neri, M., Grosser, H., & Zschau, J. (2009): Simultaneous magma and gas eruptions at three volcanoes in southern Italy: An earthquake trigger?. *Geology*, *37*(3), 251-254.

Weaver, S. D., Bradshaw, J. D. and Adams, C. J. (1991): Granitoids of the Ford Ranges, Marie Byrd Land, Antarctica, in Thomson, M. R. A., Crame, J. A. and Thomson, J. W., eds., *Geological Evolution of Antarctica*, Cambridge, Cambridge University Press, 345-351

Weaver, S. D., Storey, B. C., Pankhurst, R. J., Mukasa, S. B., Divenere, J. and Bradshaw, J. D. (1994): Antarctic-New Zealand rifting and Marie Byrd Land lithospheric magmatism linked to ridge subduction and mantle plume activity. - *Geology* *22*: 811- 814.

Wilson, D. S., Jamieson, S. S., Barrett, P. J., Leitchenkov, G., Gohl, K., & Larter, R. D. (2012): Antarctic topography at the Eocene-Oligocene boundary. *Palaeogeography, Palaeoclimatology, Palaeoecology*, *335*, 24-34.

Yakymchuk, C., Brown, M., Brown, C., Siddoway, C.S., Fanning, C.M., Korhonen, F.J. (2015): Paleozoic evolution of western Marie Byrd Land, Antarctica.- *Geological Society of America Bulletin*, doi:10.1130/B31136.1 (pre-pub available online prior to print publication).



Figure 1: The continent of Antarctica. The red box delineates the study area within Marie Byrd Land.

[http://www.pgc.umn.edu/maps/antarctic/id/ANT\\_REF-MP2015-001](http://www.pgc.umn.edu/maps/antarctic/id/ANT_REF-MP2015-001)

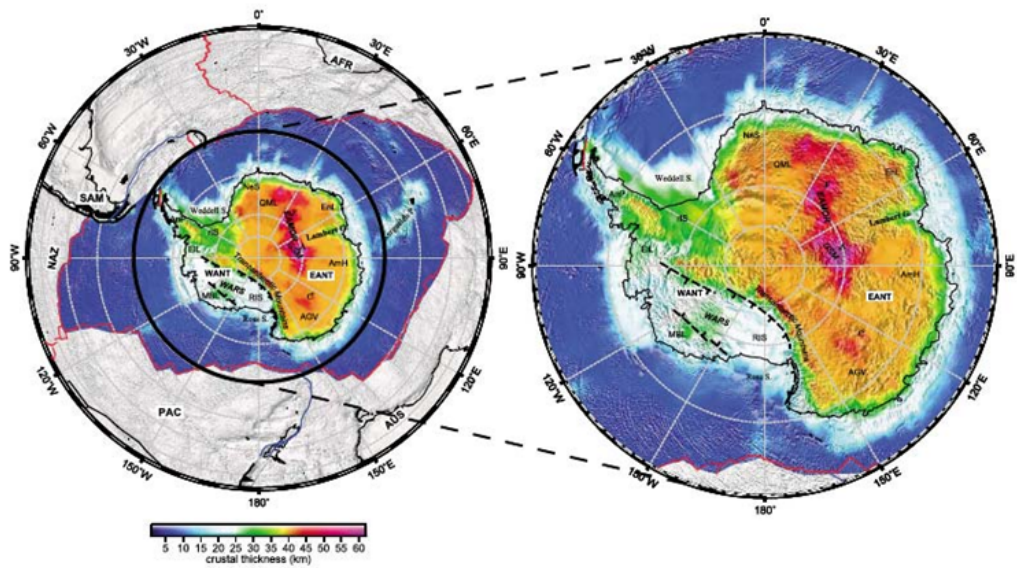


Figure 2: A crustal thickness map of the Antarctic continental plate displaying the contrast in crustal thickness between East and West Antarctica. Figure from An et al (2014)

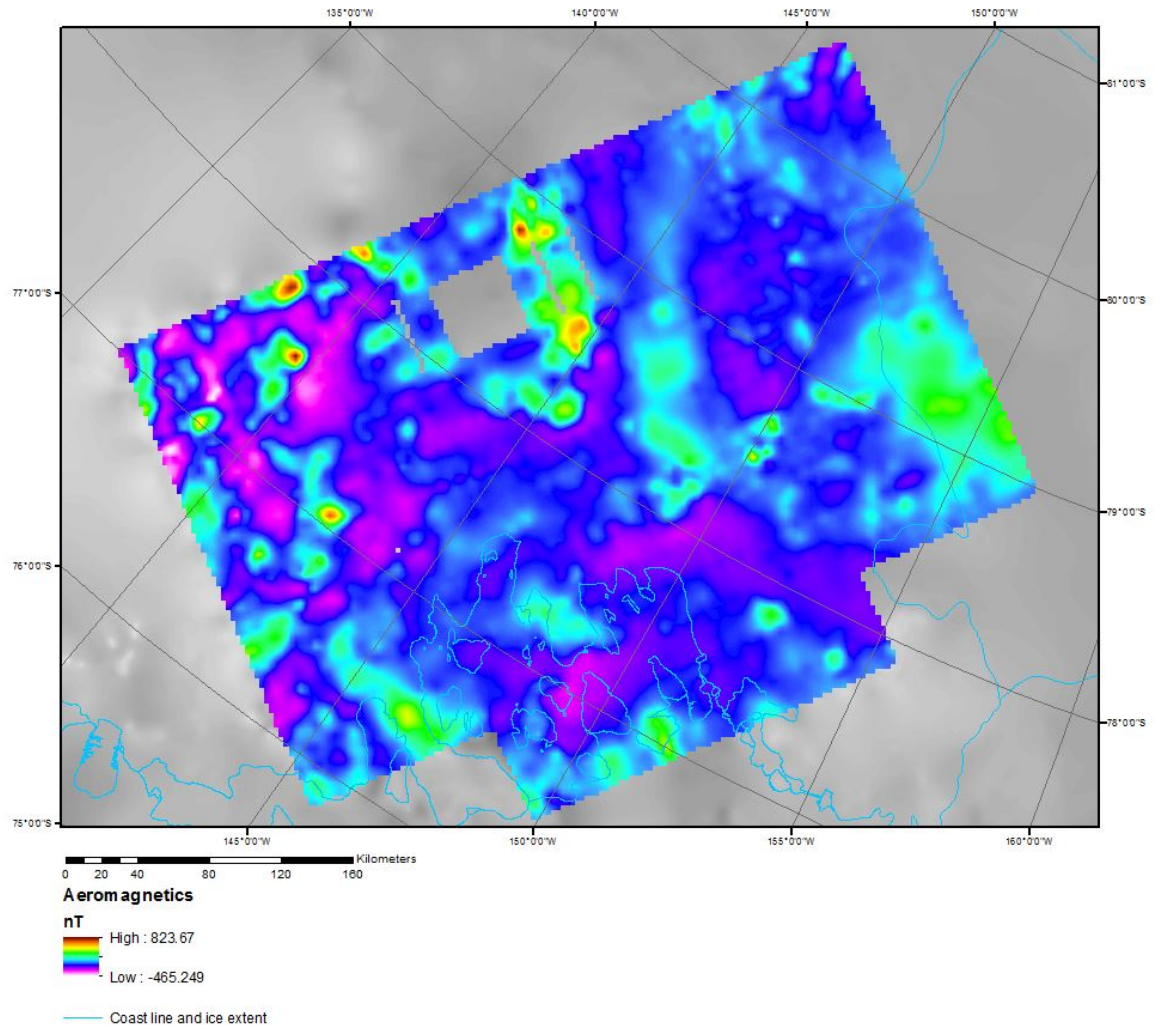


Figure 3a: Total magnetic intensity from aerogeophysical survey collected by SOAR.

<http://www-udc.ig.utexas.edu/external/facilities/aero/data/>

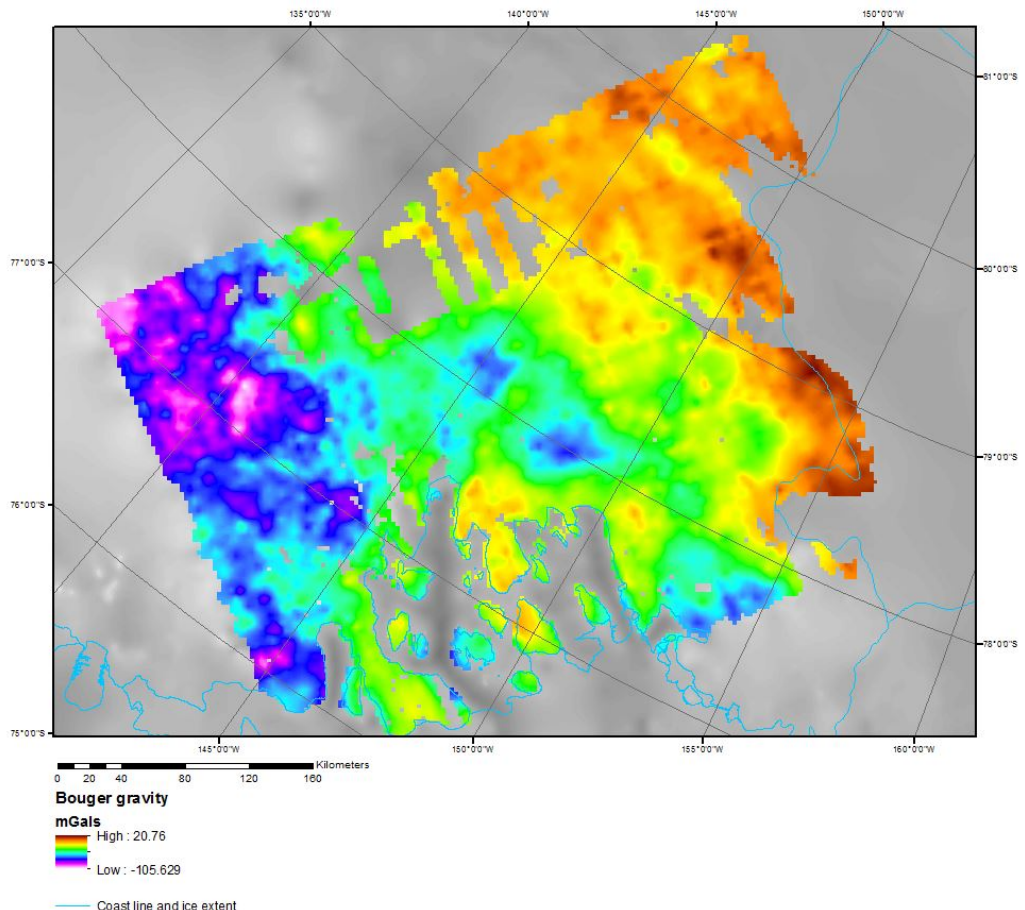


Figure 3b: Bouger gravity from aerogeophysical survey collected by SOAR.

<http://www-udc.ig.utexas.edu/external/facilities/aero/data/>

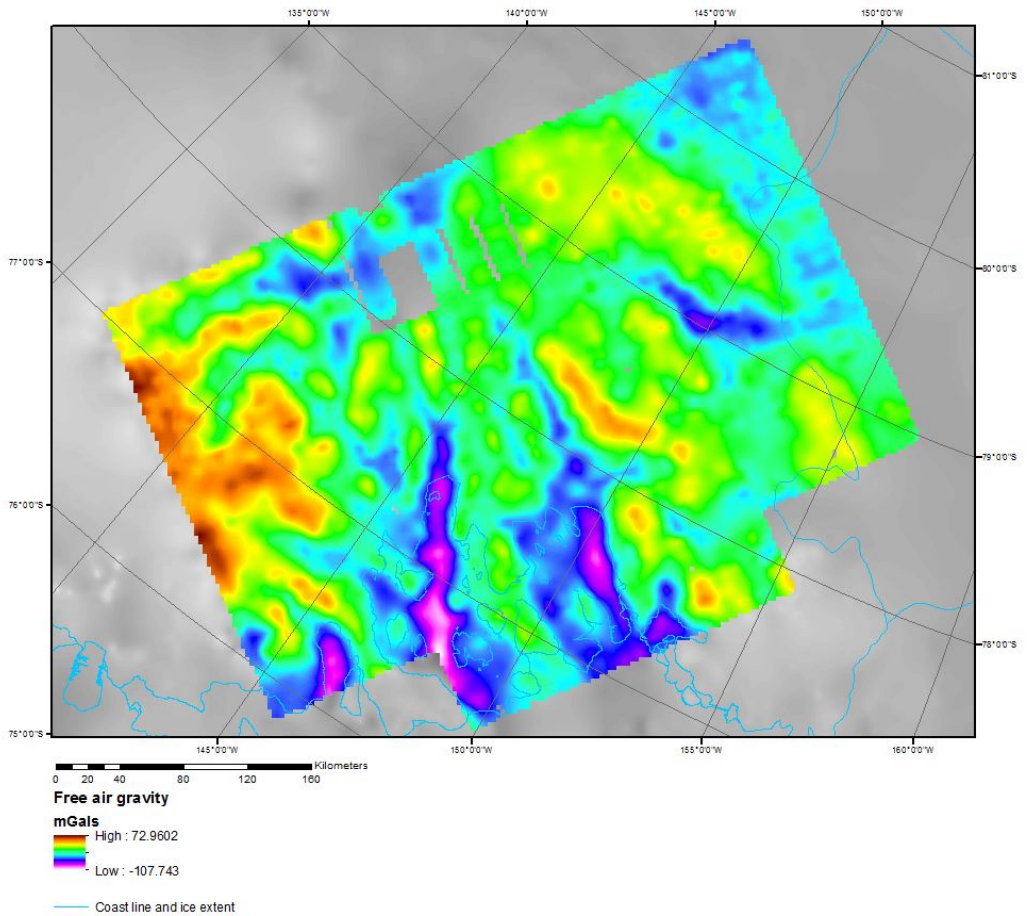


Figure 3c: Free air gravity from aerogeophysical survey collected by SOAR.  
<http://www-udc.ig.utexas.edu/external/facilities/aero/data/>

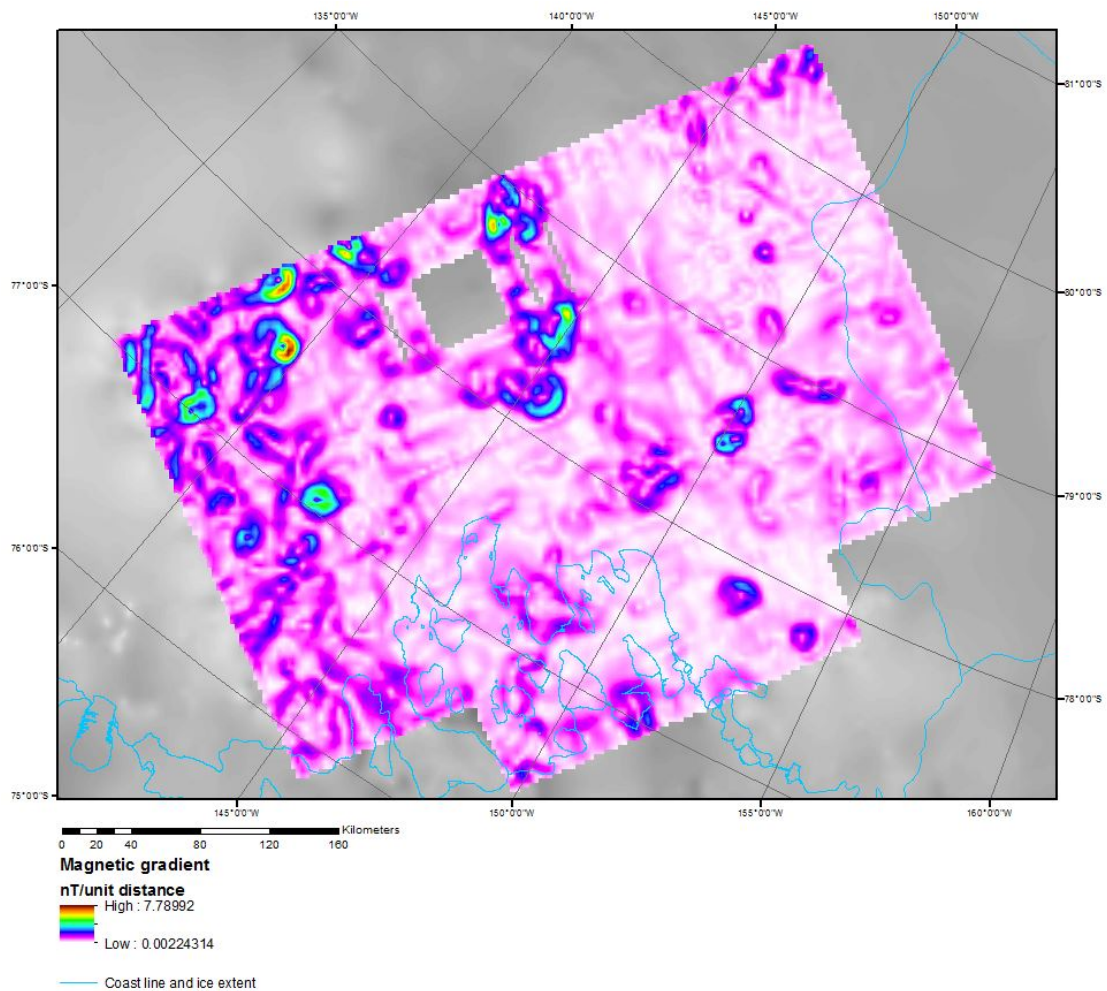


Figure 3d: Magnetic gradient derived from aerogeophysical survey collected by SOAR. Produced using the slope 3D Analyst tool in ArcMap.  
<http://www-udc.ig.utexas.edu/external/facilities/aero/data/>

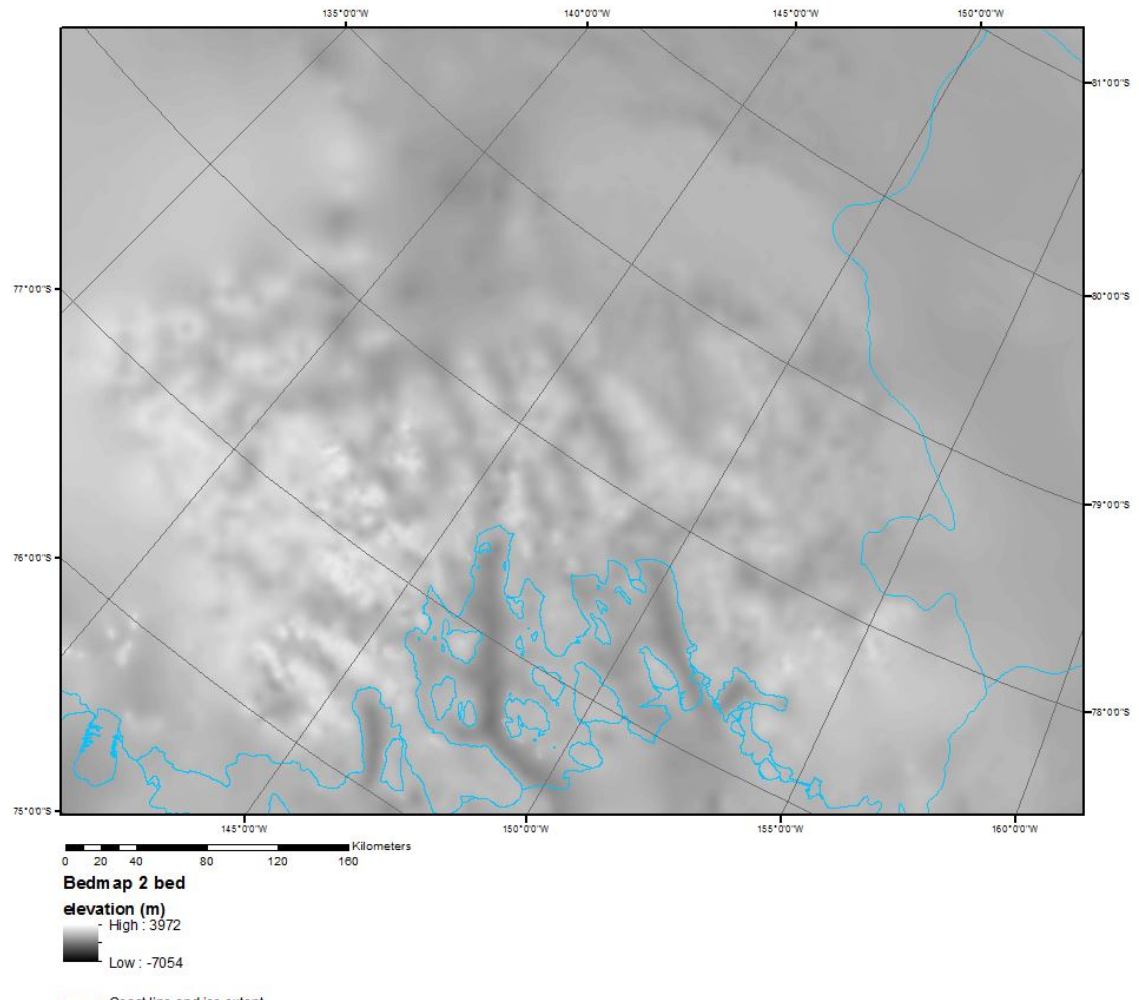


Figure 3e: Bed surface data from aerogeophysical survey collected by SOAR. These data were compiled into Bedmap 2.  
<http://www-udc.ig.utexas.edu/external/facilities/aero/data/>;  
<https://www.bas.ac.uk/project/bedmap-2/>

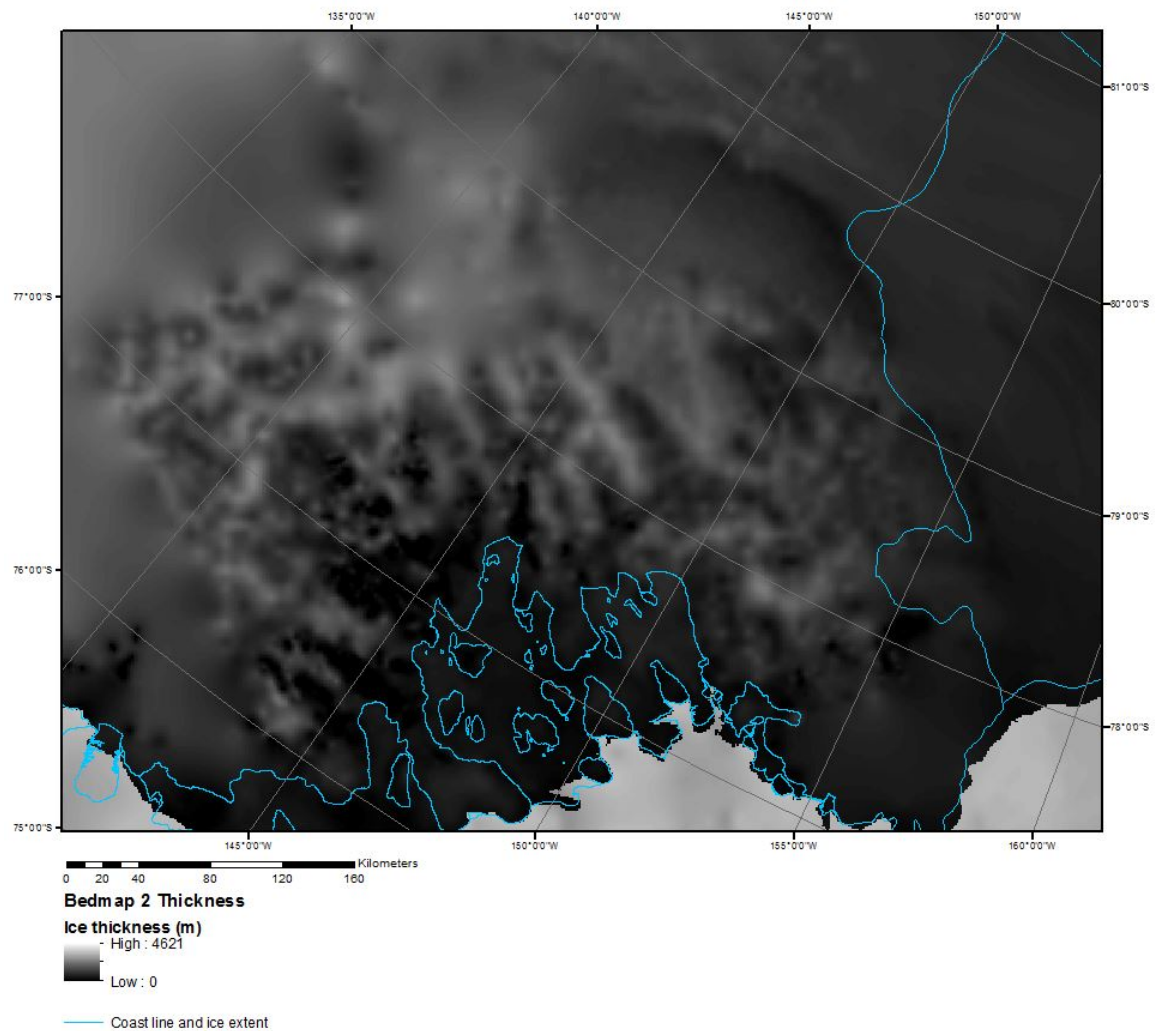


Figure 3f: Ice thickness data from aerogeophysical survey collected by SOAR. These data were compiled into Bedmap 2.

<http://www-udc.ig.utexas.edu/external/facilities/aero/data/>;

<https://www.bas.ac.uk/project/bedmap-2/>

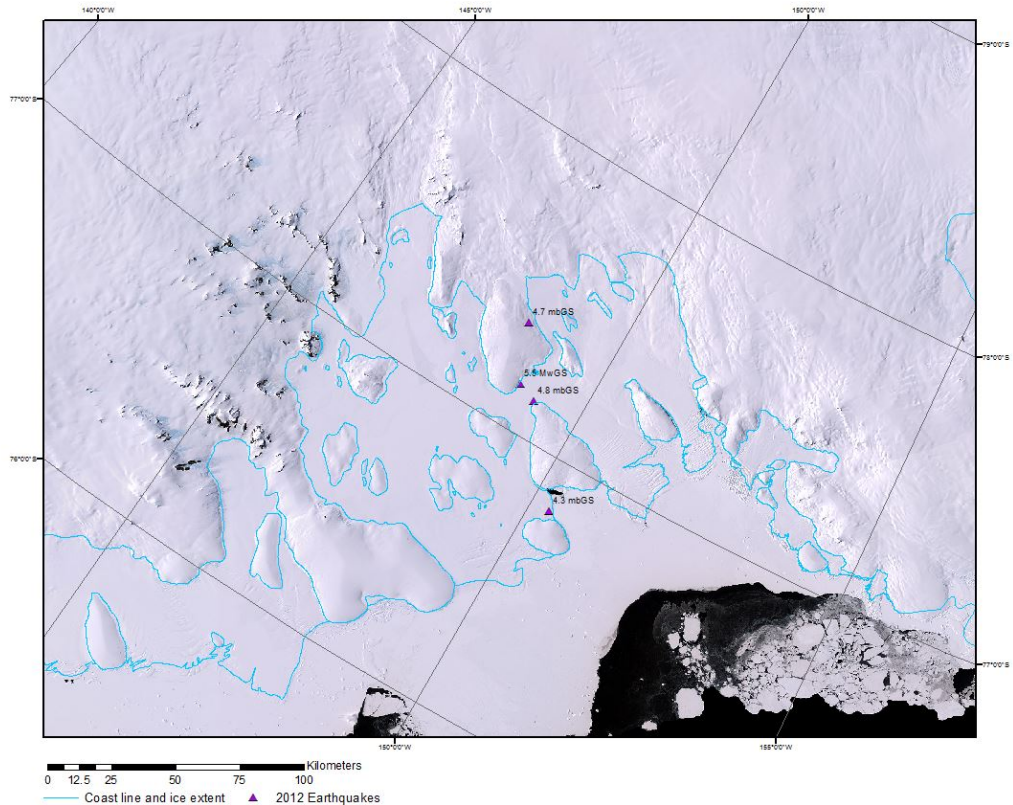


Figure 4: The locations of the four moderate magnitude earthquakes on continental crust in 2012.

[http://earthquake.usgs.gov/earthquakes/eventpage/usp000jm6p#general\\_summary](http://earthquake.usgs.gov/earthquakes/eventpage/usp000jm6p#general_summary); <http://LIMA.usgs.gov>

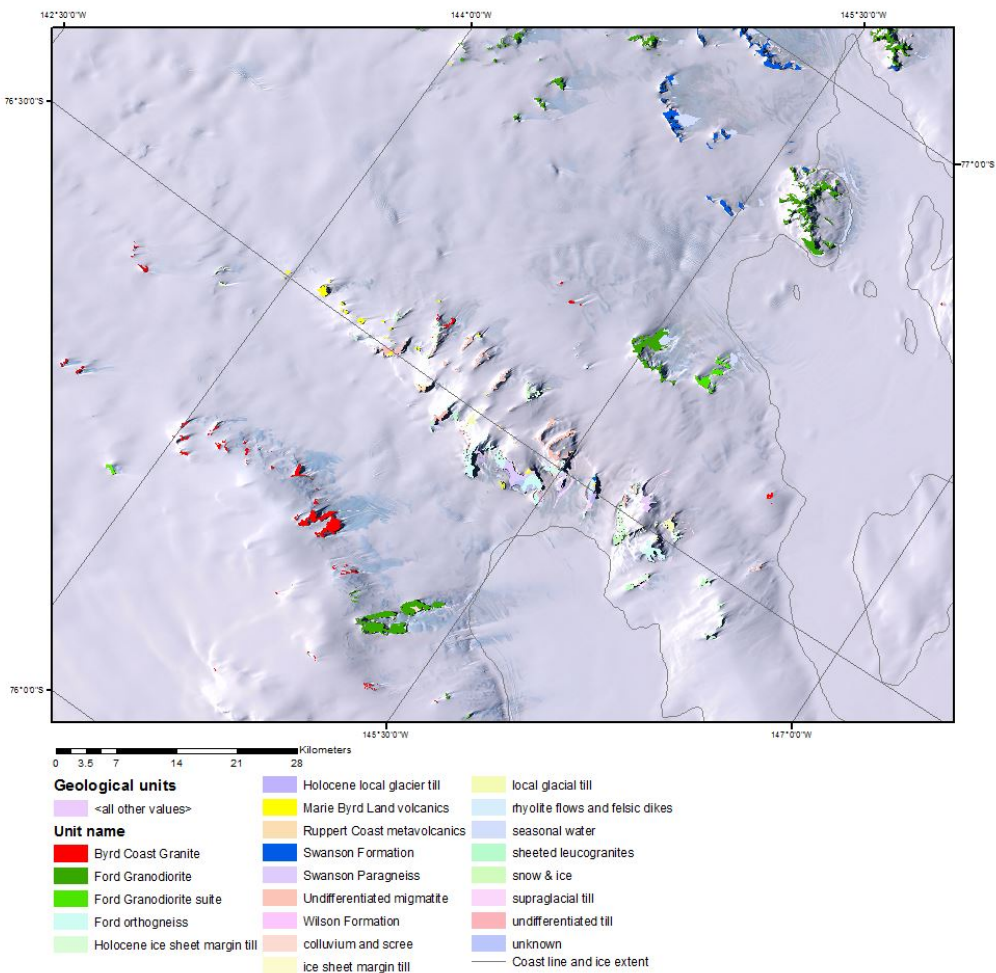


Figure 5: A sample of the outcropping geology of the Fosdick and Phillips Mountains rendered at 1:250,000 scale.

<http://LIMA.usgs.gov>

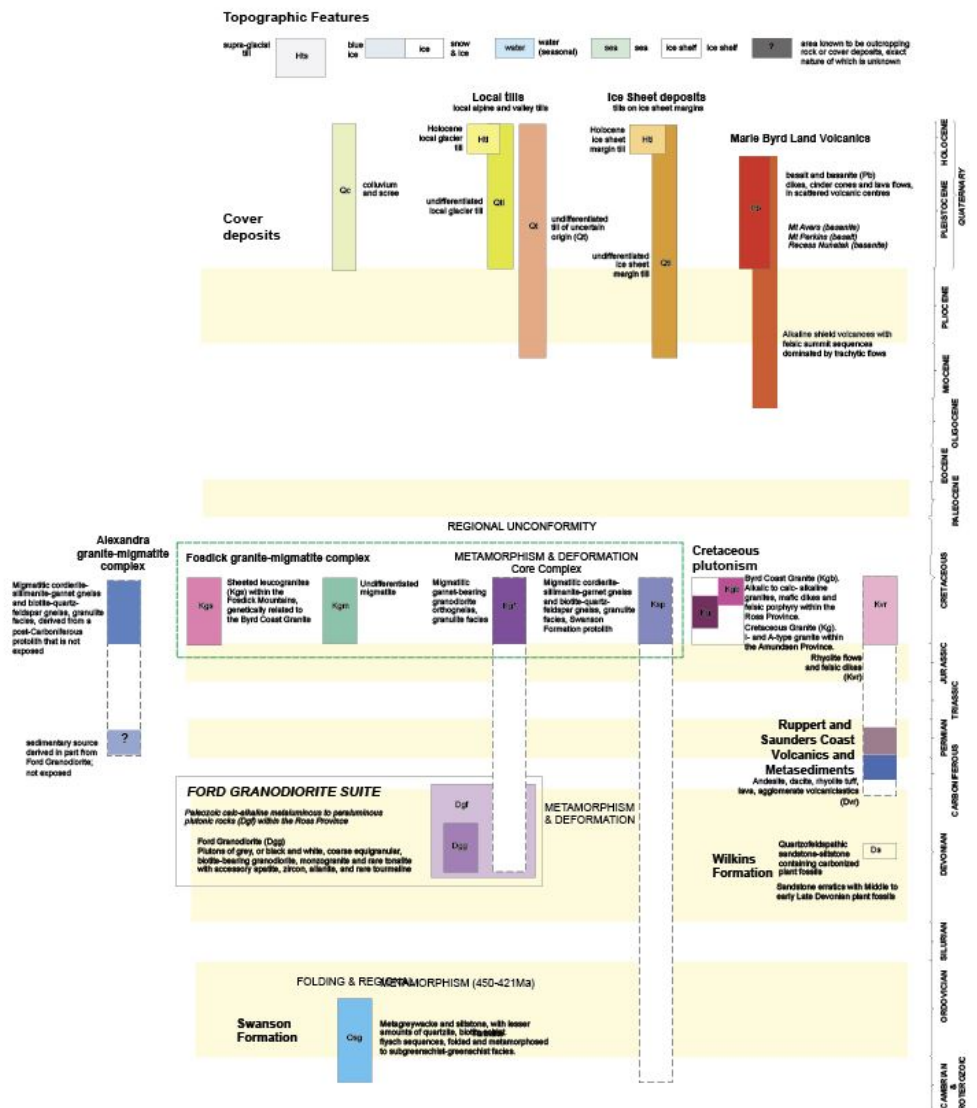


Figure 6: The geological units of the Ford Ranges and Edward VII Peninsula arranged lithostratigraphically.



Figure 7: One limb of the large scale folding in the Swanson Formation. Photo by C. Siddoway.

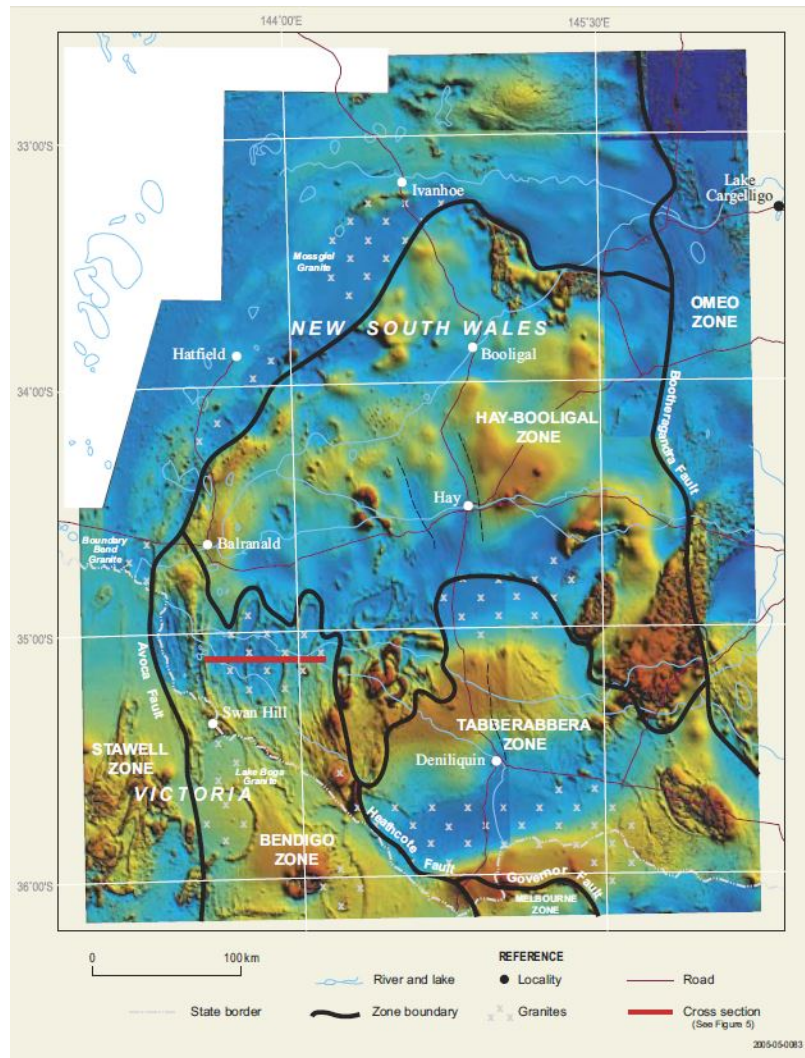


Figure 8: S-type granitoids in the Murray Basin identified in Hallett et al. (2005) by their negative signature in total magnetic intensity and bouger gravity data.



Figure 9: Digital Globe imagery available in Google Earth displaying glacial till.

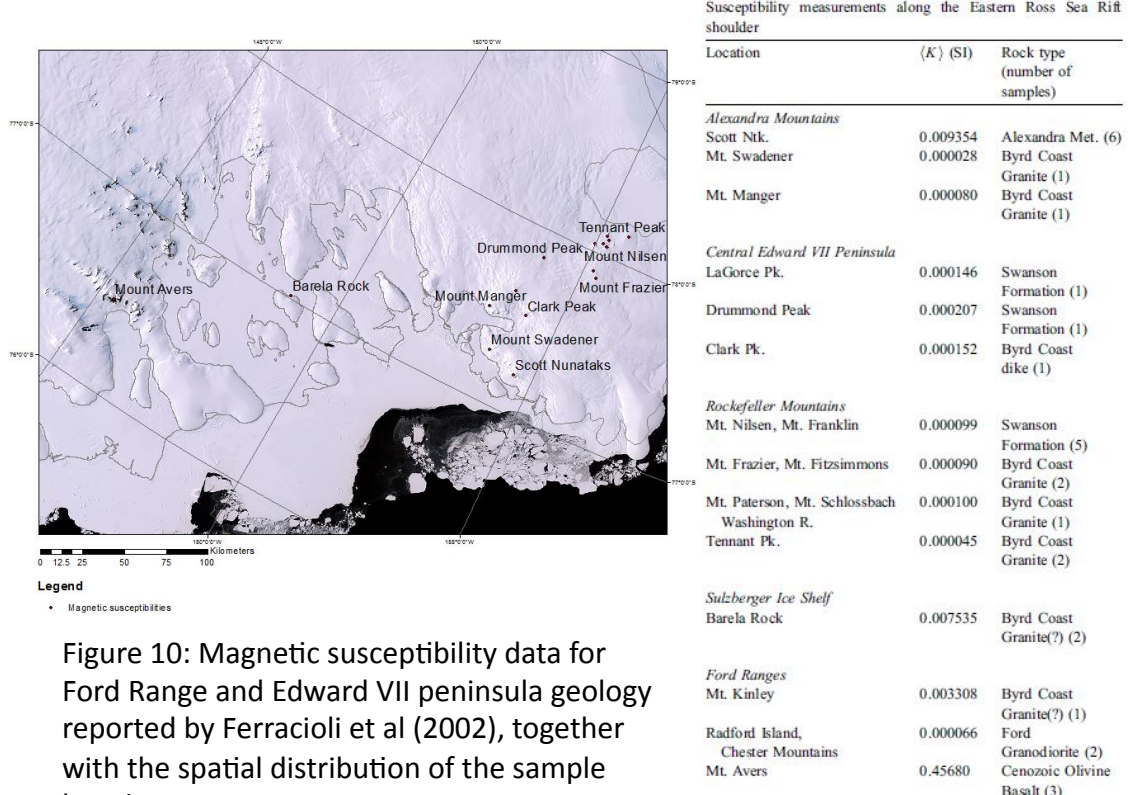


Figure 10: Magnetic susceptibility data for Ford Range and Edward VII peninsula geology reported by Ferracioli et al (2002), together with the spatial distribution of the sample locations.

<http://LIMA.usgs.gov>

High-grade rocks of the Alexandra Mountains and Cenozoic mafic volcanic rocks of the Ford Ranges are highly magnetic. Swanson Formation and Byrd Coast Granite are only weakly magnetic.

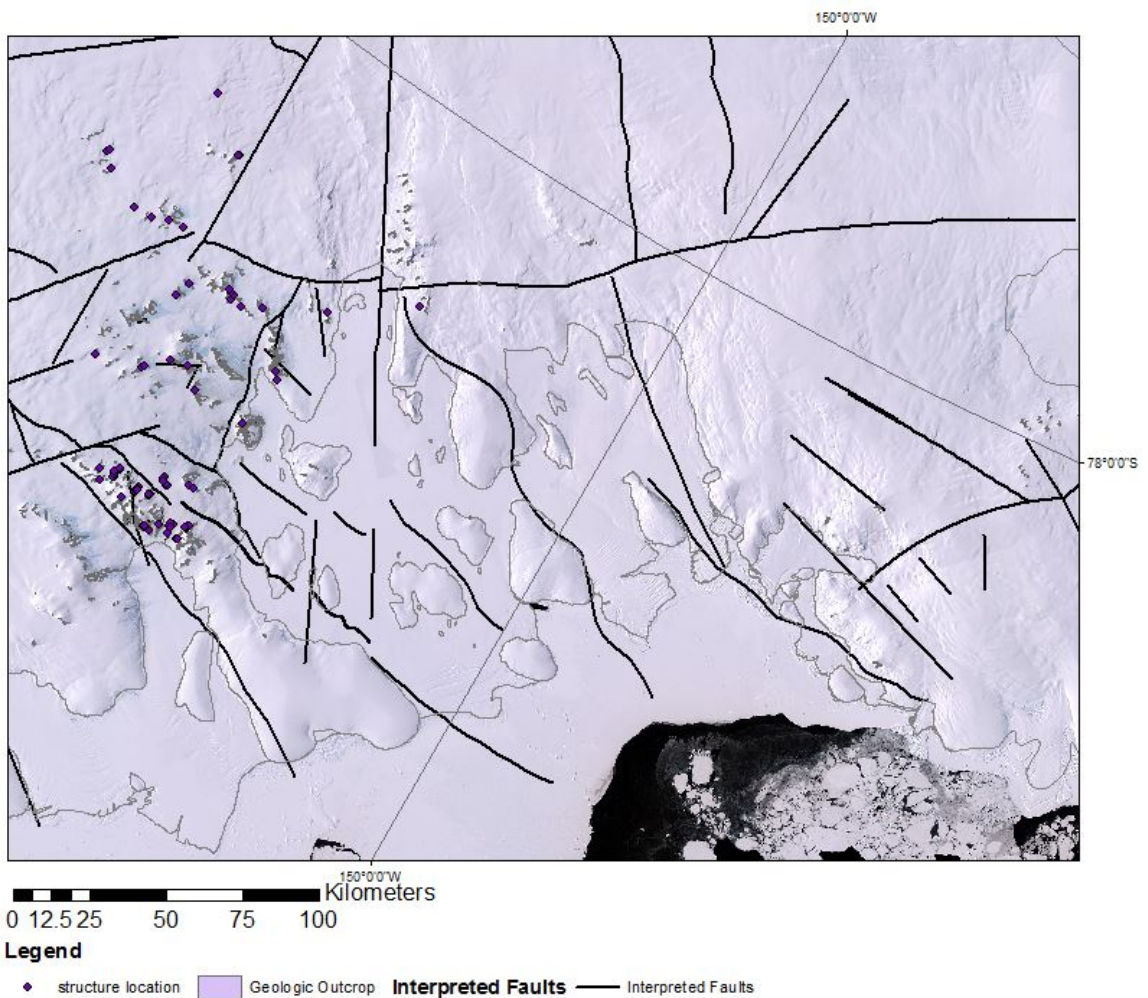


Figure 11: The Geological dataset of the Ross Province. Basemap imagery from <http://LIMA.usgs.gov>

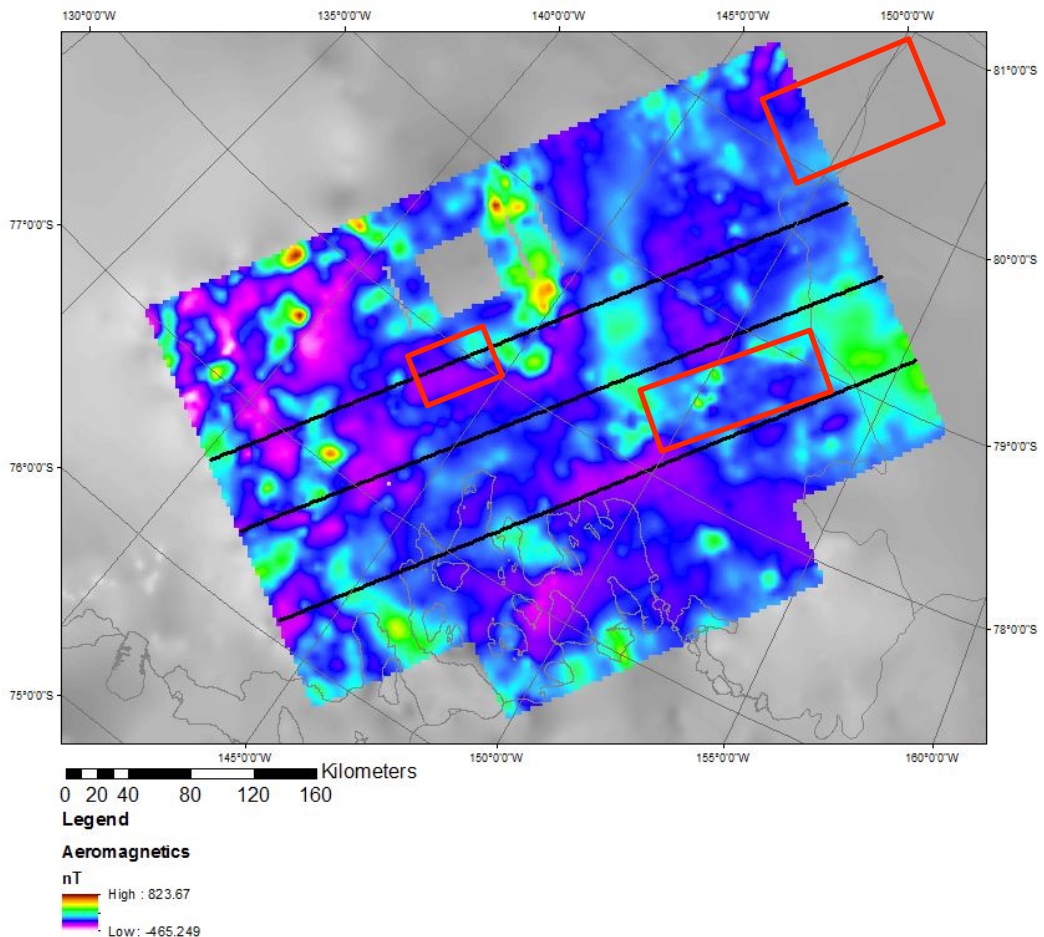
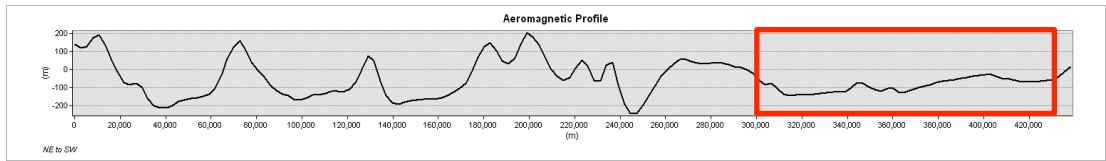
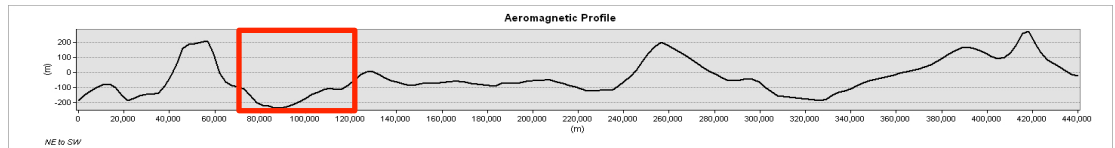


Figure 12 : Large magnetically “quiet” regions of the magnetic anomaly map.

<http://www-udc.ig.utexas.edu/external/facilities/aero/data/>  
<https://www.bas.ac.uk/project/bedmap-2/>



**A**



**B**

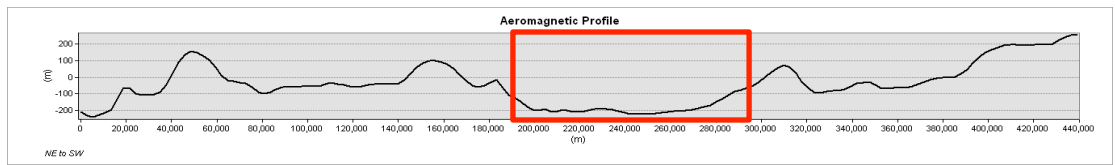


Figure 12b: The same large magnetically “quiet” regions of the magnetic anomaly map shown in profile.

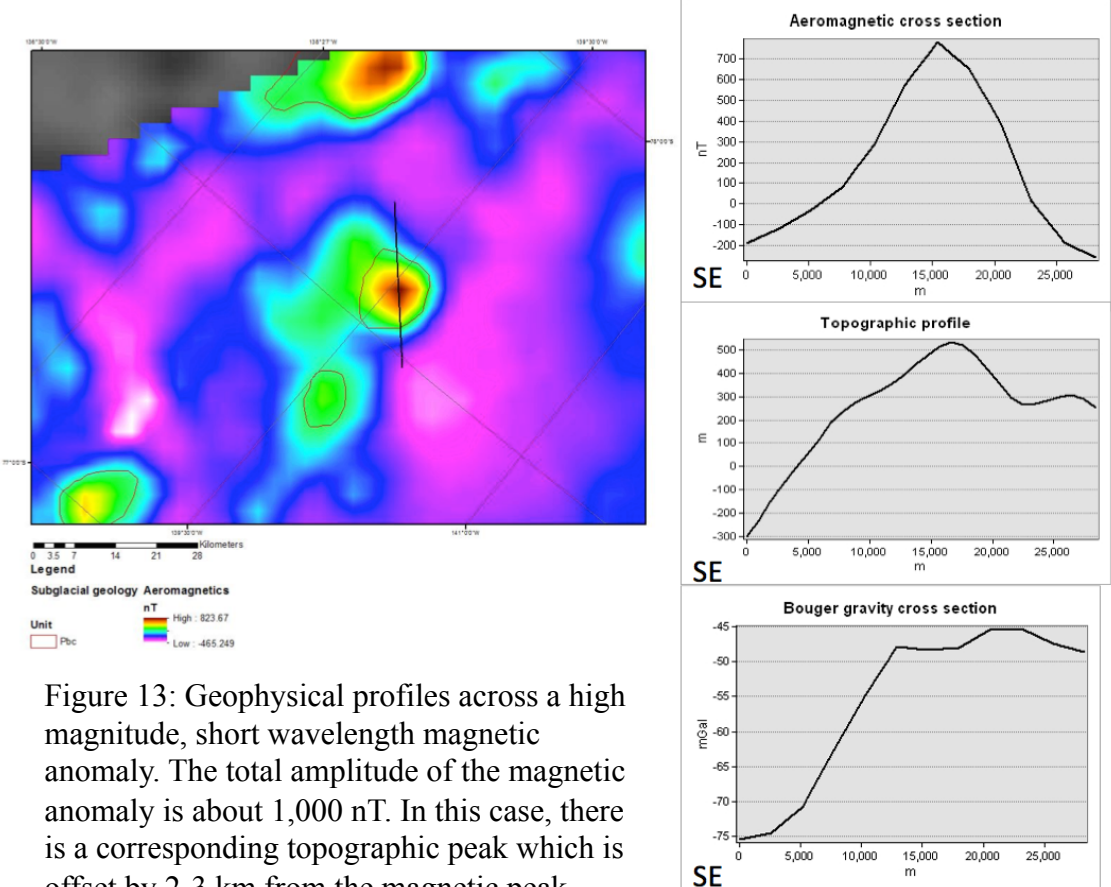


Figure 13: Geophysical profiles across a high magnitude, short wavelength magnetic anomaly. The total amplitude of the magnetic anomaly is about 1,000 nT. In this case, there is a corresponding topographic peak which is offset by 2-3 km from the magnetic peak. There is no discernible matching peak in the Bouger gravity. The total magnetic anomaly is approximately 15 km across.

[http://www-udc.ig.utexas.edu/external/  
facilities/aero/data/](http://www-udc.ig.utexas.edu/external/facilities/aero/data/)

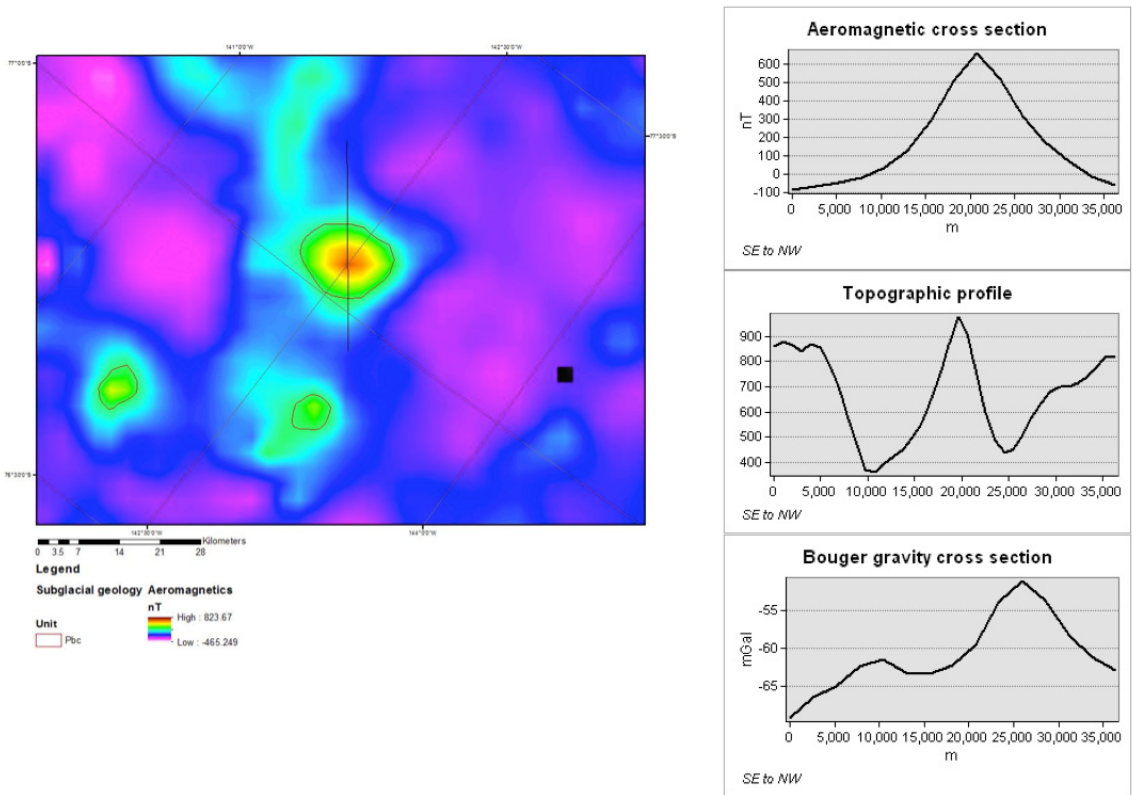


Figure 14: Geophysical profiles across another high magnitude, short wavelength magnetic anomaly. The total amplitude of the magnetic anomaly is about 800 nT. In this case, there is a corresponding topographic peak which is offset by 2-3 km from the magnetic peak. While there is a peak in the Bouger gravity with a 10 mGal amplitude, it is offset from the magnetic peak by 5 km and is likely unrelated. The total magnetic anomaly is approximately 15 km across.

<http://www-udc.ig.utexas.edu/external/facilities/aero/data/>

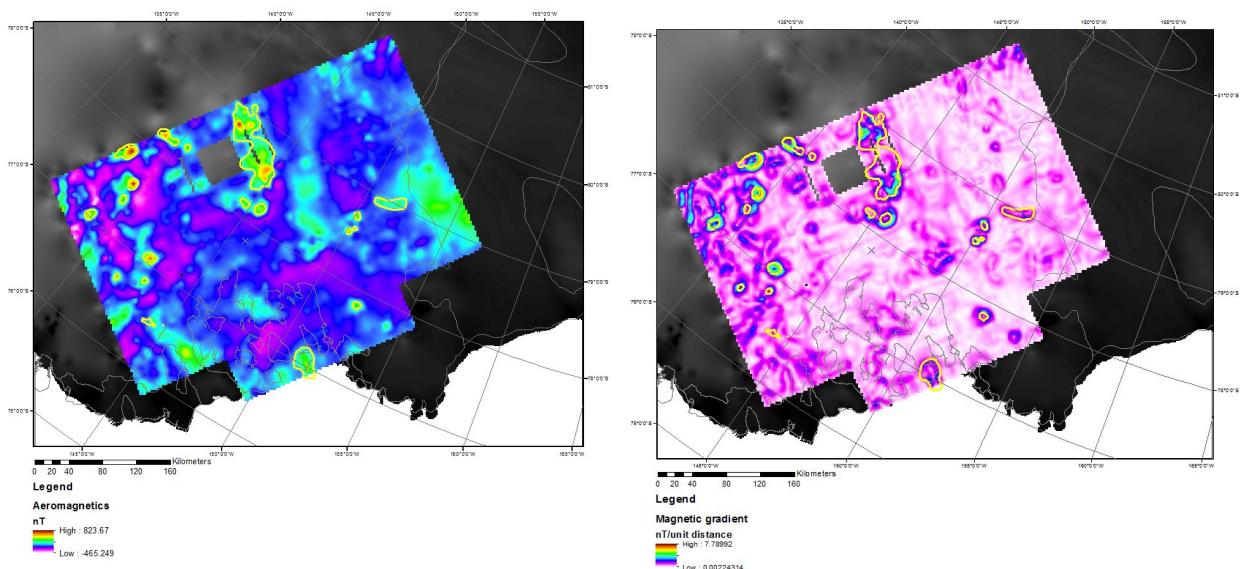


Figure 14: The spatial distribution of all magnetic anomalies interpreted to indicate Pleistocene-age volcanic features. The majority of the features are located in the northeast corner of the study area although there is a notable collection in the East-central region.

<http://www-udc.ig.utexas.edu/external/facilities/aero/data/>

<https://www.bas.ac.uk/project/bedmap-2/>

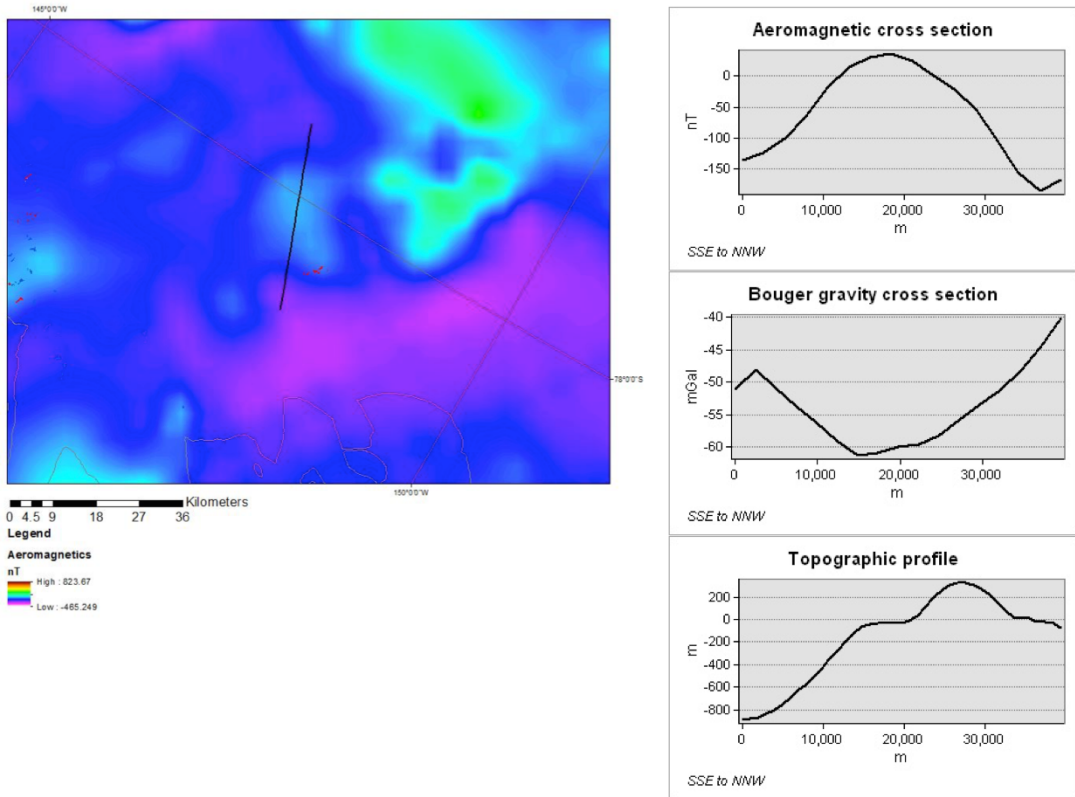


Figure 15: Geophysical profiles across a medium magnitude, intermediate wavelength magnetic anomaly. The total amplitude of the magnetic anomaly is about 180 nT. In this case, there is no corresponding topographic peak. There is no discernible matching peak in the Bouger gravity. The total magnetic anomaly is approximately 30 km across.

<http://www-udc.jg.utexas.edu/external/facilities/aero/data/>

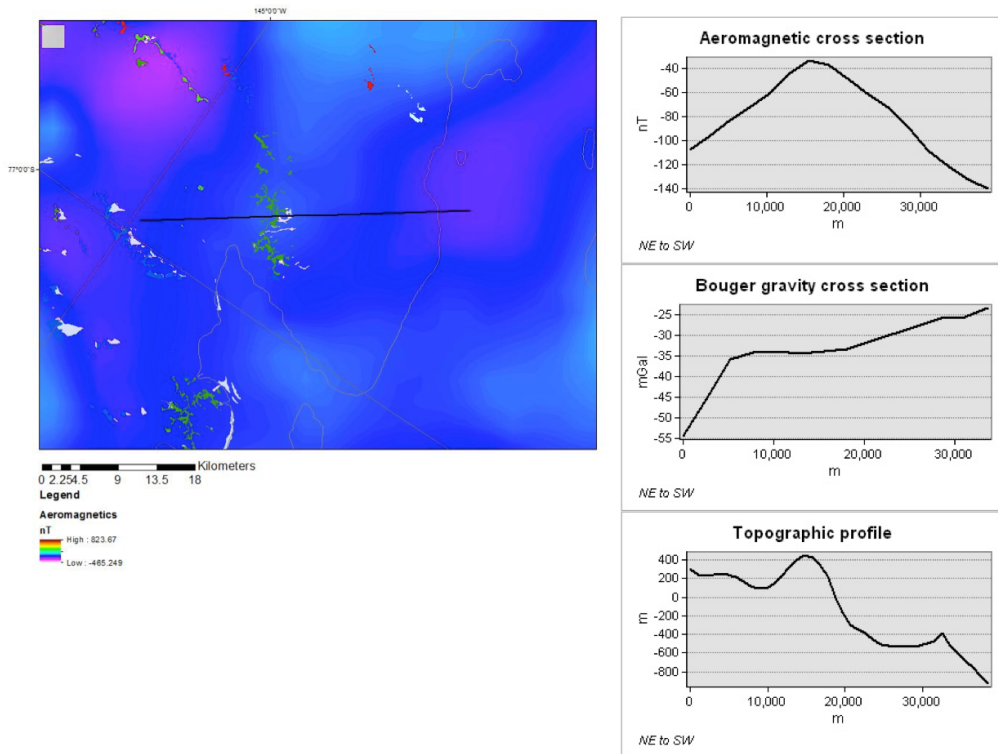


Figure 16: Geophysical profiles across a medium magnitude, intermediate wavelength magnetic anomaly. The total amplitude of the magnetic anomaly is about 180 nT. In this case, there is a corresponding topographic peak offset by 1-2km. There is no discernible matching peak in the Bouger gravity. The total magnetic anomaly is approximately 30 km across.

<http://www-udc.ig.utexas.edu/external/facilities/aero/data/>

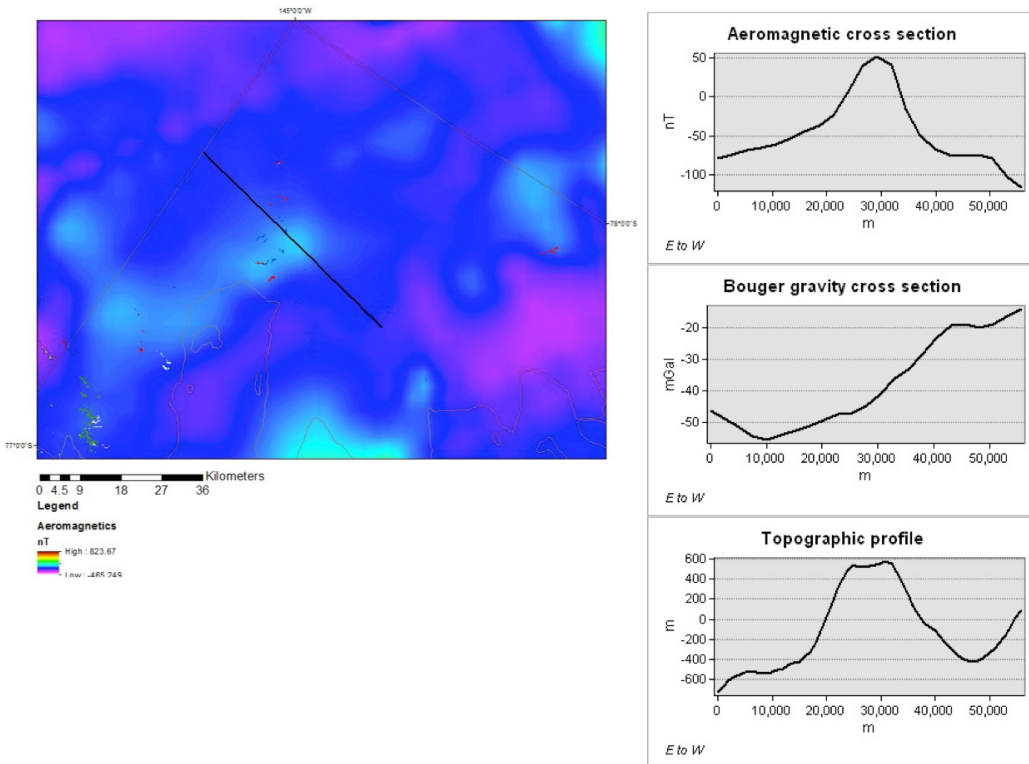


Figure 17: Geophysical profiles across a medium magnitude, intermediate wavelength magnetic anomaly. The total amplitude of the magnetic anomaly is about 180 nT. In this case, there is no corresponding topographic peak. There is no discernible matching peak in the Bouger gravity. The total magnetic anomaly is approximately 18 km across. This anomaly is narrower with a higher gradient than those in figures 14 and 13. This is likely due to a body that is nearer to the surface and possibly with higher magnetic susceptibility.

<http://www-udc.ig.utexas.edu/external/facilities/aero/data/>

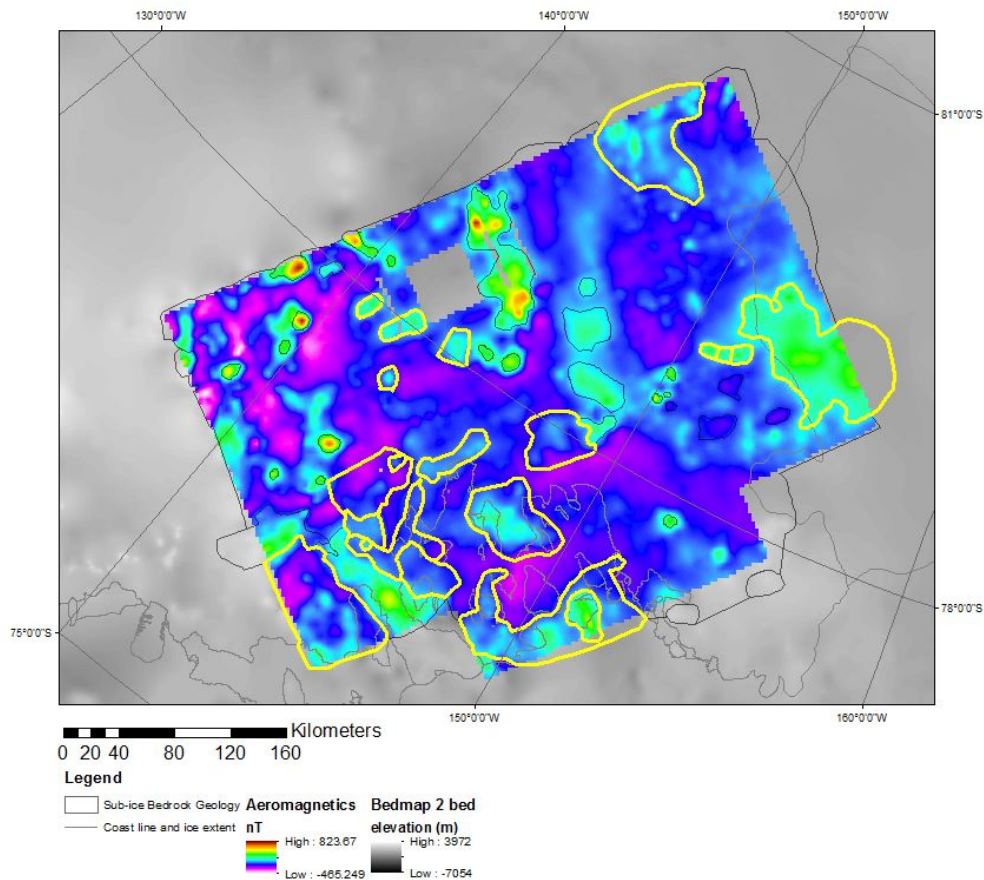


Figure 18: The total extent of intrusive bodies in the Ross Province.  
<http://www-udc.ig.utexas.edu/external/facilities/aero/data/>  
<https://www.bas.ac.uk/project/bedmap-2/>

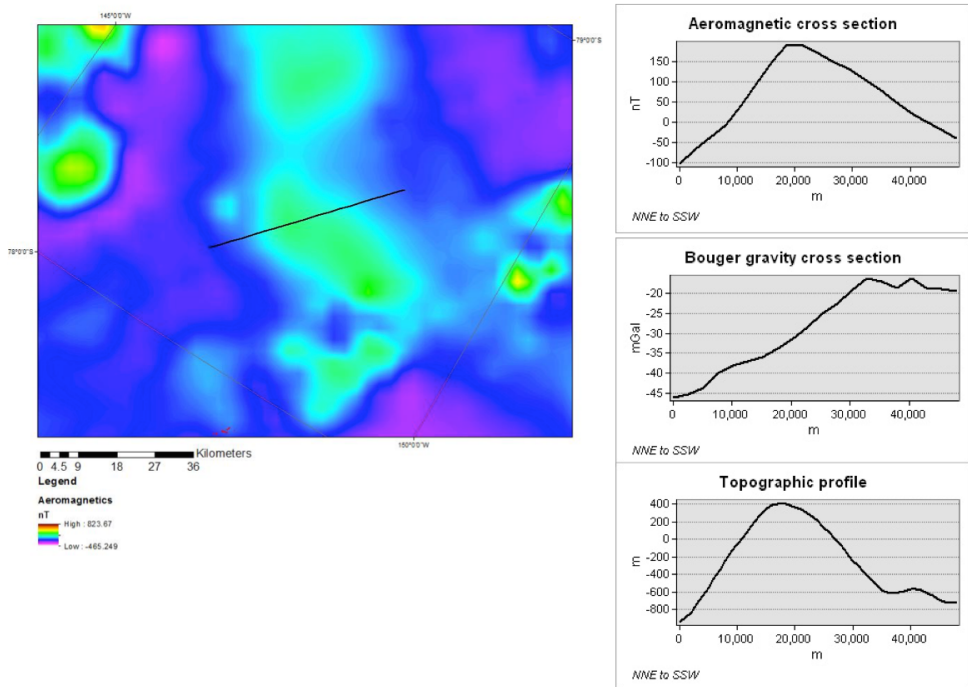


Figure 19: Geophysical profiles across a proposed metamorphic core complex.

<http://www-udc.ig.utexas.edu/external/facilities/aero/data/>

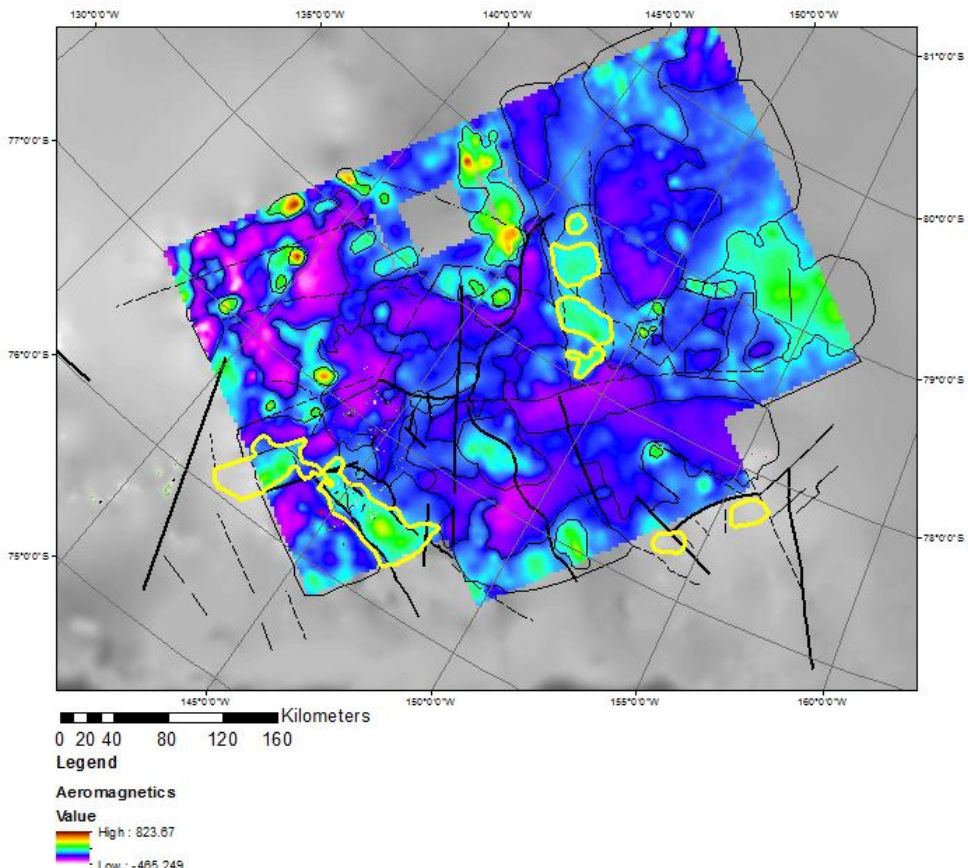


Figure 20: the spatial distribution of geophysical anomalies interpreted to be metamorphic core complexes.

<http://www-udc.ig.utexas.edu/external/facilities/aero/data/>

<https://www.bas.ac.uk/project/bedmap-2/>

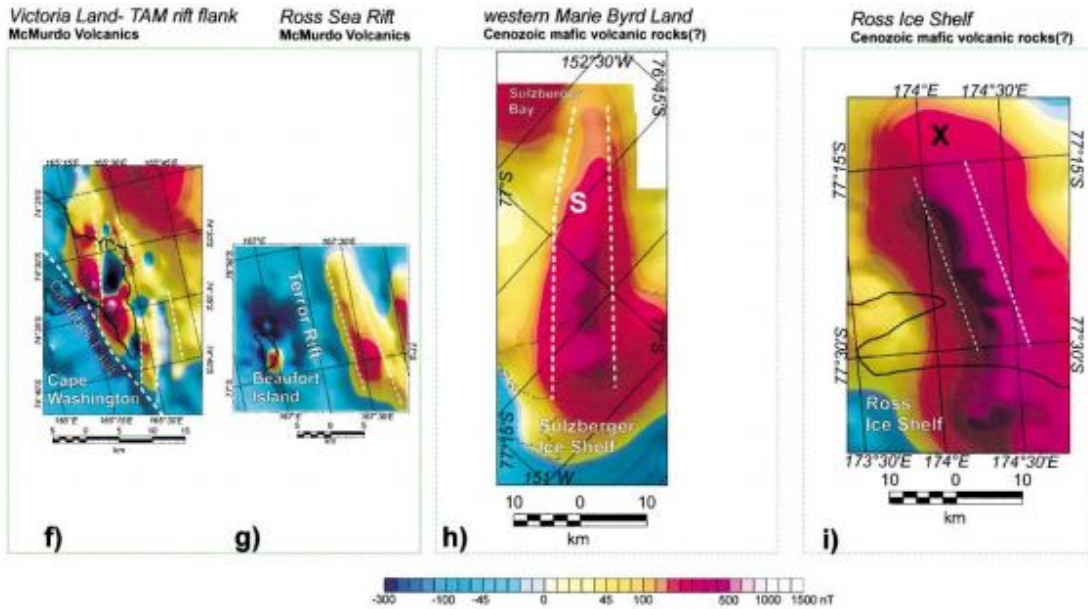


Figure 21: Comparative analysis of elongate, high amplitude magnetic anomalies by Ferraccioli et al., (2002).

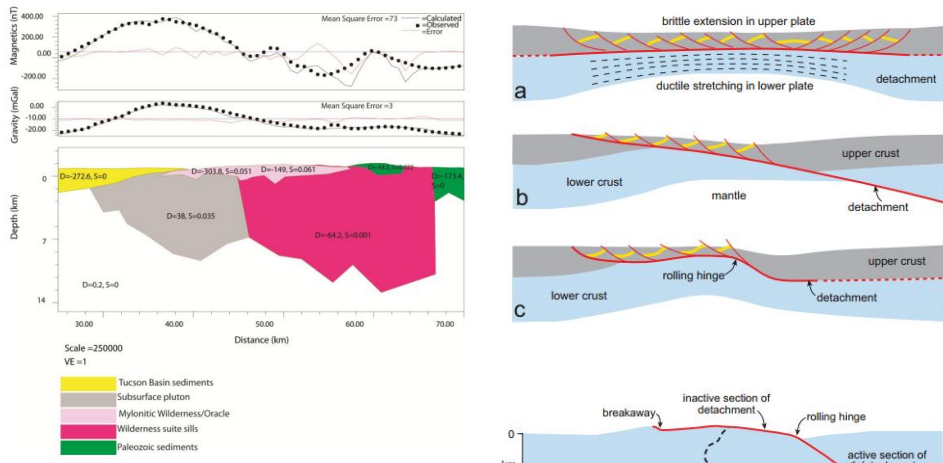


Figure 8.

Figure 22: Examples of models of metamorphic core complexes from Terrien (2012) and Platt et al. (2014).

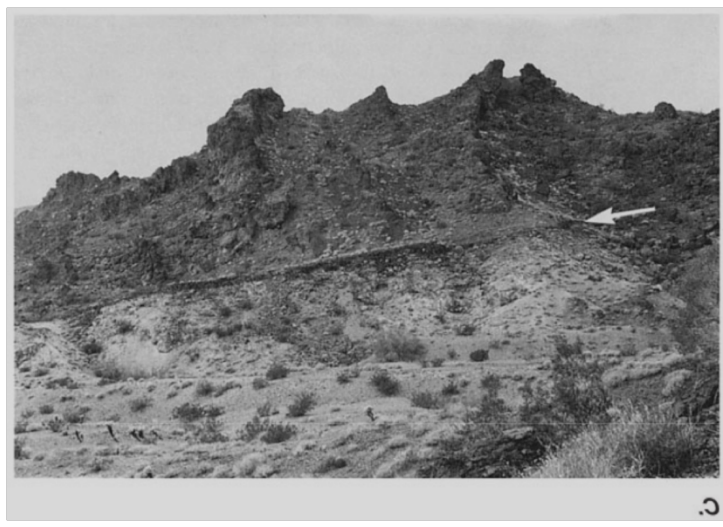
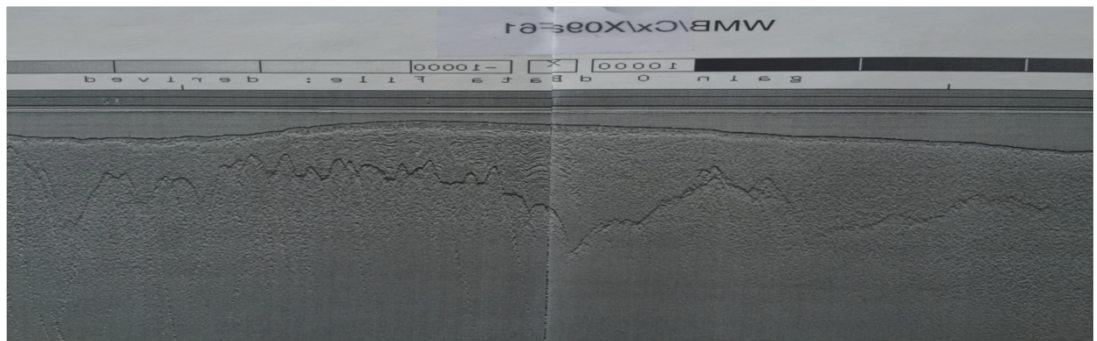


Figure 23: The Whipple detachment fault: a possible analogue for a hypothesized metamorphic core complex. Photo from Twiss and Moores (2007).

<http://www-udc.ig.utexas.edu/external/facilities/aero/data/>

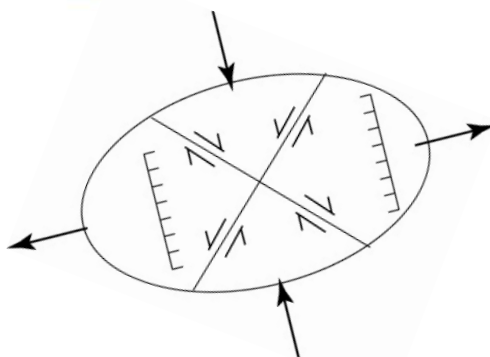
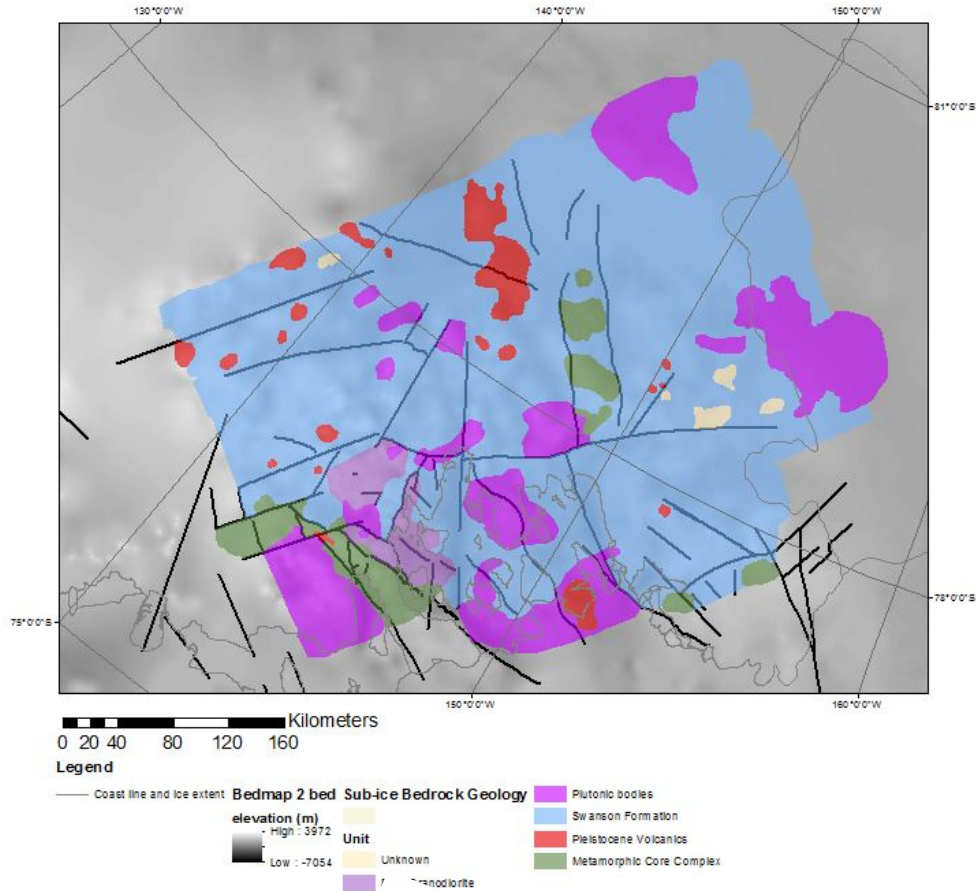


Figure 24: The strain ellipse for a extensions direction of ~65 NE with faults that conform to these kinematics.

<https://www.bas.ac.uk/project/bedmap-2/>